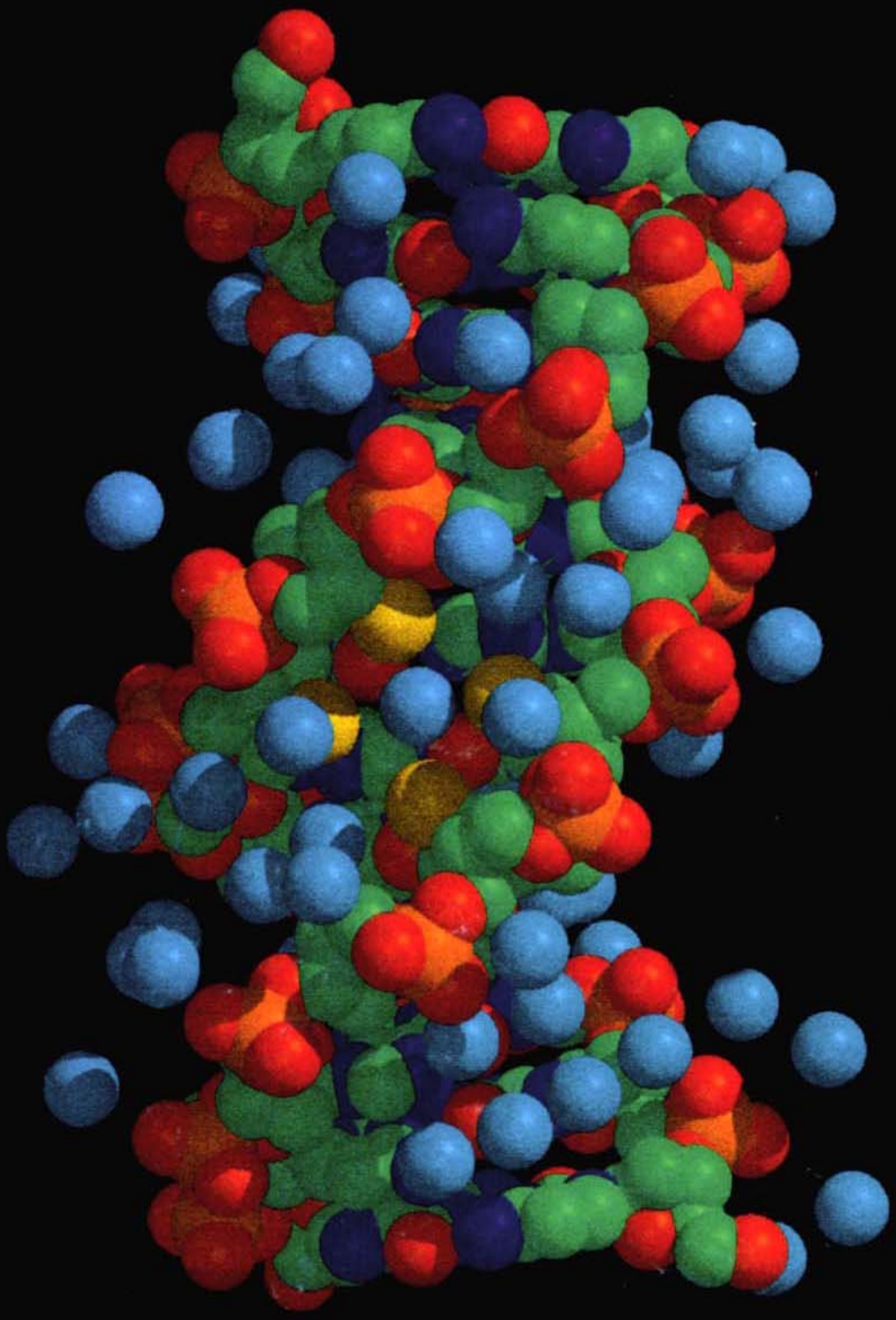

Hydration of the B-DNA duplex [d(CGCGAAT^{Me}T^{Me}CGCG)]$_2$ (T^{Me} = carbocyclic 6´-α-methylthymidine). Water molecules are shown as light blue spheres; the carbon atoms of the α-CH_3 substituents in the modified thymidine residues are represented by yellow spheres.

Structural Aspects of Nucleic Acid Analogs and Antisense Oligonucleotides

Martin Egli*

Hybridization of complementary oligonucleotides is essential to highly valuable research tools in many fields including genetics, molecular biology, and cell biology. For example, an antisense molecule for a particular segment of sense messenger RNA allows gene expression to be selectively turned off, and the polymerase chain reaction requires complementary primers in order to proceed. It is hoped that the antisense approach may lead to therapeutics for treatment of various diseases including cancer. Areas of active research in the antisense field focus on the mechanisms of cellular uptake of antisense molecules and their delivery to specific cell sites, an improved understanding of how these molecules inhibit the production of proteins, as well as the optimization of the chemical stability of antisense molecules and the thermodynamic stability of the duplexes they form with the mRNA targets. The last two issues in particular have prompted chemists to launch an extensive search for oligonucleotide analogs with improved binding properties for hybridization with RNA and higher resistance toward nuclease degradation. During the last years this research has resulted in a flurry of new chemical analogs of DNA and RNA with modifications in the sugar–phosphate backbone as well as in the nucleobase sites. However, to date little effort has been directed toward uncovering the exact origins of the gain or loss in stability when nucleic acid analogs bind to RNA. Although large amounts of thermodynamic data have been collected, the structural perturbations induced by the modifications in hybrid duplexes are only poorly understood. For many modified oligonucleotides the compatibility of protection, coupling, and deprotection chemistry with standard DNA and RNA synthesis protocols makes it now possible to generate modified nucleic acid fragments or mixed oligonucleotides containing modifications at selected sites in quantities suitable for three-dimensional structure investigations. Such studies should reveal the structural origins of the observed changes in affinity and specificity of binding for particular modifications and may guide the development of second- and third-generation antisense molecules. In addition, the availability of a previously unimaginable variety of modified building blocks and the investigation of their structures provides the basis for a deeper understanding of the native DNA and RNA structures. This contribution will summarize the results of X-ray crystallographic structure determinations of modified nucleic acid fragments conducted in our laboratory during the last three years and the insights gained from them.

Keywords: crystal structure analysis · DNA · hydrogen bonding · RNA

1. Introduction

The precisely ordered strings formed by the four nucleotide bases adenine (A), thymine (T), guanine (G), and cytosine (C), and the formation of complementary, hydrogen-bonded A–T and G–C base pairs provide the foundation for gene structure and expression. In chromosomes the DNA usually exists in the form of an antiparallel double helix composed of the sense strand and the antisense strand. Pairing specificity is the underlying principle of all biological information transfer—replication, recombination, transcription, and translation. In bacteria and viruses hybridization between sense RNA and antisense RNA is a common mechanism for regulation as well as inhibition of gene activity. Both replication and transcription were shown to be controlled by such mechanisms in prokaryotes.[1–4] In order to control replication of the *E. coli* plasmid ColE1, a sense–antisense RNA complex is formed between two complementary loop structures.[5, 6] These initial observations of a natural mechanism to suppress genetic information via nucleic acids were followed by a decade of intense exploration of the possibilities and limits of the antisense approach.

Antisense RNA need not necessarily be administered through expression vectors, but can be injected into cells in the form of short synthetic oligonucleotides. In addition, it was first shown by Zamecnik and coworkers that DNA can also be utilized to effectively inhibit protein expression.[7, 8] Messenger RNA in the unprocessed and processed state is not the only possible target; interference with the protein expression pathway can in

[*] Prof. M. Egli
Department of Molecular Pharmacology and Biological Chemistry
Northwestern University Medical School
303 East Chicago Avenue
Chicago, IL 60611-3008 (USA)
Fax: Int. code +(312)503-0796
e-mail: m-egli@nwu.edu

  0570-0833/96/3517-1895 $ 15.00+.25/0

principle also occur at the gene level. However, this approach is thus far restricted largely to homopurine target sites that allow triplex formation with the antigene strand.[9-11] More effective control of gene expression may be exhibited by antisense RNAs with functional properties, for example *trans*-acting hammerhead ribozymes that can cleave a target message after the sequence UH (H = A, C, or U) and will thus not only inhibit but actively degrade the sequence.[12, 13]

The experience gathered in various areas of the antisense field during the last years has indicated several critical points that must be addressed should the antisense technology become applicable in the treatment of human diseases. These obstacles for antisense drug development will only be briefly addressed here; most aspects have been exhaustively treated in a series of excellent recent reviews and books.[14-33] Potential pitfalls to successful application of antisense therapeutics are the often low cellular uptake and the insufficient chemical stability of natural and chemically modified oligonucleotides against degradation by various nucleases. Once resistant against nucleases and efficiently delivered, a modified oligonucleotide may not sufficiently discriminate between a chosen target and other sites. Further complications can arise from the fact that most of the modified DNAs and RNAs do not induce RNase H-mediated cleavage of mRNA,[34] that folding of cellular RNAs into secondary and tertiary structures may render the selected target sites inaccessible, and that the antisense strand and target may not be found in the same location within the cell.

It is anticipated that appropriate chemical modification of oligonucleotides may help overcome some of these problems. In particular, modifications may lead to improved hybridization properties, nuclease resistance, and cell permeation. The structural framework of DNA and RNA allows a multitude of chemical modifications on the phosphate backbone and on the sugar and base moieties. First-generation analogs based on these three constituents include the phosphorothioates,[35, 36] the methylphosphonates,[37, 38] and a range of O2′-modified oligonucleotides.[39-42] The current variety of analogs is overwhelming, and the interested reader is referred to other sources such as the previously mentioned reviews.[14-33]

Among the newer generation of backbone modifications are 3′-allylethers and 3′-allylsulfides,[43] amides,[44] amines,[45] carbon chains,[46] formacetals and thioformacetals,[47, 48] guanidinium linkages,[49] 5′-methyl DNA and RNA,[50] phosphoramidates,[51] phosphorodithioates,[52] sulfides,[53] sulfonamides,[54] and sulfones.[55] The analogs with modifications on the sugar portion comprise carbocyclic compounds,[56, 57] L-2′-deoxyriboses,[58] and hexoses.[59-61] Oligonucleotides in which the pyrimidine rings have propyne substituents at C5 display promising features for antisense applications,[62] and the peptide nucleic acids (PNAs) introduced in 1994 are the analogs with the highest divergence from the native nucleic acids.[63]

The abundant number of modifications is in stark contrast to the handful of detailed structural studies of analogs using either solution NMR or modeling methods. Among those analyzed are amide-linked DNA,[64, 65] formacetal DNA,[66, 67] thioformacetal DNA,[68] urea-linked DNA,[69] phosphorodithioate DNA,[70] 2′-*O*-methyl RNA,[71] 2′-5′-linked RNA,[72] a PNA–RNA duplex,[73] and a PNA–DNA duplex.[74] In addition, structural investigations conducted with PNAs include the crystal structure of a triple-stranded nucleic acid complex, consisting of a homopurine DNA nonamer and two homopyrimidine PNA nonamers, in which the latter strands are linked through six amino acids.[75] Much more structural work will be necessary to interpret the thermodynamic stability data of oligonucleotide modifications, and to begin to understand the complex interplay between enthalpic and entropic effects, including factors such as conformational preorganization, hydration, salt concentration, and cooperativity.[76, 77]

Beyond the search for therapeutically feasible antisense compounds, recent progress in the chemical alteration of DNA and RNA provides numerous opportunities to probe nucleic acid structure[78, 79] as well as interactions between proteins and nucleic acids.[80]

2. The Structures of DNA and RNA

RNA differs from DNA by the additional hydroxyl group at the 2′-position in the ribose. This seemingly subtle difference has important consequences for the chemical and structural properties of RNA and its biological role. DNA is normally a double-stranded molecule, while RNA is single-stranded and can adopt complex folding motifs with a range of structural elements such as double-helical stems, bulges (with unpaired bases), hairpin loops, and pseudoknots.[81] DNA has been observed in two general classes of right-handed duplexes with antiparallel orientation of strands, the A- and the B-form (Fig. 1). One should keep in mind, however, that nucleic acid structure is polymor-

M. Egli was born in 1961 in Schaffhausen, Switzerland. He studied chemistry at the ETH-Zürich, obtaining his diploma in 1984 and his PhD in 1988 under Professors V. Prelog, J. D. Dunitz, and M. Dobler for the structural investigation of the enantioselectivity of simple receptors such as tartrates toward biologically interesting substrates including α-amino alcohol salts. He then joined Professor A. Rich's research group at MIT in Cambridge, MA (USA), where he studied the structure of nucleic acids, their complexes with drugs, and the properties of chimeric RNA–DNA molecules by using X-ray crystallographic methods. In 1992 he moved to the Organic Chemistry Laboratory at the ETH to pursue independent research on the structures of chemically modified DNA and RNA. This account summarizes research conducted by the author while at the ETH. In the fall of 1995 Egli joined the faculty of the Northwestern University Medical School in Chicago, IL (USA), as an assistant professor.

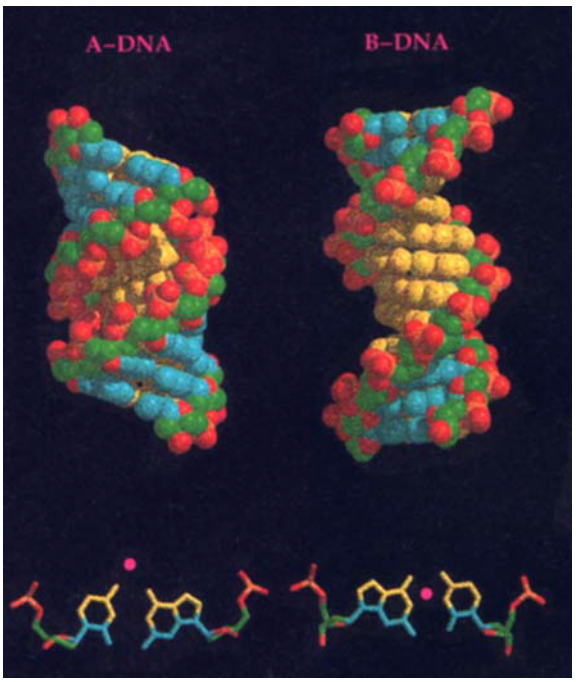

Fig. 1. Top: van der Waals models of the two basic right-handed double-helical conformations of DNA (RNA adopts an A-type duplex). The edges of the base pairs in the major groove are yellow and those in the minor groove are cyan. Bottom: Relative orientations of base pair and helix axis (pink) for A-DNA -RNA (left) and B-DNA (right) in axial projections.

phic; other stable conformations, although not necessarily double-stranded, exist.[82] In this discussion we will analyze DNA and RNA analogs in their right-handed duplex states.

Double-stranded RNA adopts an A-type conformation exclusively and is relatively inflexible. On the other hand, double-stranded DNA displays considerable conformational polymorphism and can exist in a range of conformations featuring both A- and B-like characteristics. These are influenced by the base sequence,[83] hydration state,[84, 85] the lattice contacts in a particular crystal form,[86-89] and the binding motif and interface in protein-DNA complexes,[90] among others. The crystal structure determinations of more than one hundred DNA fragments[91-94] and some four dozen protein-DNA complexes[95-98] have yielded a detailed picture of the DNA double helix. The impact of X-ray crystallography on our understanding of DNA structure and its biological role has thus far not been matched for RNA—apart from the early success with the elucidation of the tRNA structure—because of difficulties in generating highly pure RNA samples.

A- and B-type duplexes are characterized by very different topologies (Fig. 1). The major groove of the A-duplex is narrow and deep, and the minor groove is wide and shallow. The major groove of the B-duplex is wide but not as deep as that of the A-form, and the minor groove is narrower than that in the A-form but of similar depth. The A-duplex has a larger diameter and the helical axis is located in the major groove, whereas it runs through the centers of base pairs in the B-duplex. Several other features distinguish the two duplexes. The base pairs are inclined relative to the helix axis in the A-type duplex, but are more or less normal to the axis in the B-type. Phosphate groups are more closely spaced within strands in the former duplex (5.9 Å on average, B-DNA 7 Å, Fig. 2). These differences in geometry are a direct consequence of the conformational flexibility of the sugar moiety. In the A-DNA form the sugars adopt a so-called C3′-*endo* pucker, and in the B-DNA form the sugar conformation is of the C2′-*endo* type. Sugar conformations that fall into direct neighbor ranges of these two in the furanose pseudo-rotation phase cycle are also observed, but do not drastically change the overall conformations.

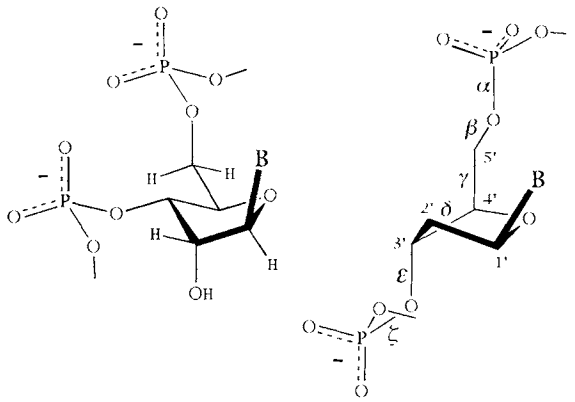

Fig. 2. Schematic diamond-lattice representations of the sugar-phosphate backbone conformations in A- and B-type duplexes. In A-DNA -RNA the six torsion angles α, β, γ, δ, ε, and ζ adopt the conformations sc^-, ap, sc^+, sc^+, ap, sc^-, respectively; in B-DNA, the conformations are sc^-, ap, sc^+, ap, ap, and sc^+. B = nucleobase.

The geometry of the sugar-phosphate backbone of oligonucleotides can be described by six torsion angles, α, β, γ, δ, ε, and ζ; the δ angle describes the torsion angle around the ribose C4′-C3′ bond (Fig. 2). In A-type duplexes δ has a sc^+ conformation, and in B-type duplexes, its conformation is *ap*. All other torsion angles fall into the same ranges in both duplexes. Readers who are not familiar with nucleic acid structure are referred to the excellent review article by Kennard and Hunter[91] for nomenclature and definitions, as well as to Saenger's book on the principles of nucleic acid structure.[99]

3. Crystallization of Oligonucleotide Analogs

3.1. Choosing the Template Sequence and the Sites for Incorporating Modified Nucleotides

A crucial step toward the exploration of chemically modified nucleic acids by X-ray crystallography is the availability of template sequences known to produce crystals that diffract reasonably well (typically to better than 2.5 Å resolution), and the determination of the number and the locations of incorporation sites with a particular nucleotide analog that will preserve crystallization. We have established such sequences and incorporation sites for both modified DNA and RNA oligonucleotides. Scheme 1 illustrates the trial-and-error approach that was used for growing high-resolution crystals of a B-DNA template containing carbocyclic residues. With this d(CGCGAATTCGCG)

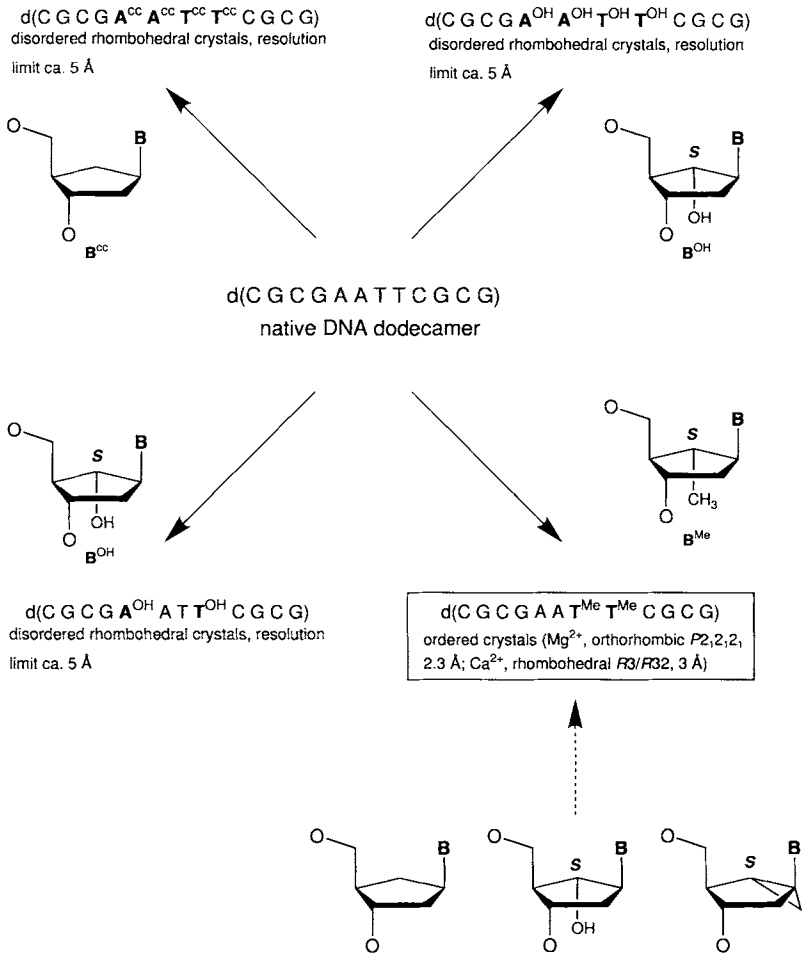

Scheme 1. Selection of incorporation sites for carbocyclic nucleotides in a B-DNA dodecamer [107] that will still yield well-diffracting crystals. Placing carbocyclic 6′-α-methylthymidines (T^{Me}) at positions 7 and 8 produced two crystal forms; the orthorhombic crystals are isomorphous with those of the native DNA oligonucleotide. Various carbocyclic analogs can now be incorporated at these sites (see bottom of scheme) with the goal of producing crystals of good diffraction quality and then comparing the structural changes.

or so-called Dickerson–Drew dodecamer, optimal crystallization results were obtained with carbocyclic analogs incorporated at locations T(7) and T(8). The dodecamer was originally selected because of its demonstrated mutation tolerance and lattice conservation in over 35 cases (NDB, Nucleic Acid Crystal Structure Data Base,[100] search December 1994).

It is now widely believed that the targeting of a particular stretch of messenger RNA with RNA analogs may hold certain advantages over the targeting with DNA analogs in terms of stability and selectivity. RNA·RNA duplexes are considerably more stable than the corresponding RNA·DNA hybrids.[101] This suggests that it is important to study RNA modifications within the context of an RNA or A-form double helix. We have relied on two template sequences for the incorporation of RNA analogs: the RNA octamer r(CCCCGGGG)[102,103] and the A-type DNA with sequence d(GCGTATACGC).[104–106]

3.2. Crystal Growth

A comparison of the conditions used to grow crystals of oligonucleotides discloses an amazing similarity between many of them. In probably more than 90% of the cases, the mother liquor components include sodium cacodylate buffer, magnesium chloride, spermine tetrahydrochloride, and 2-methyl-2,4-pentanediol (MPD) as the precipitant. At the onset of crystallization experiments with analogs, it is therefore reasonable to include these components. Obviously, such established techniques[108,109] do not always produce crystals. The conditions for growing protein crystals are considerably more diverse than those for nucleic acids. A common approach is the use of sparse matrix screens[110] that allow efficient sampling of a variety of buffers, cations, and precipitants. These screens are commercially available,[111] and modified versions have recently been applied successfully in the crystallization of medium- and large-sized RNAs .[112,113]

We have used commercial screen kits to crystallize double-helical RNA fragments. Two crystal forms of the octamer $r(C_4G_4)$ could be grown from buffers with pH values between 4.5 and 8.5 and various precipitants, including high concentrations of ammonium sulfate, low molecular weight polyethylene glycols (PEGs), MPD, and others.[102] Successful use of smaller PEGs in the crystallization of RNA oligonucleotides has also been reported by other researchers.[114] The rhombohedral crystal form of the $r(C_4G_4)$ octamer diffracts X-rays to exceptionally high resolution (better than 1.5 Å) and can also be grown from solutions containing 100–250 mM concentrations of various divalent metal cations (Mg^{2+}, Ca^{2+}, Zn^{2+}, etc.). Collection of high-resolution data with these crystals should enable investigation of the RNA binding modes of these ions. The particular arrangement of $[r(C_4G_4)]_2$ duplexes in the rhombohedral lattice displays no close packing contacts for many nucleotides. This renders the $r(C_4G_4)$ sequence an ideal crystallization template for modified RNAs with alterations at a number of sites. Attempts at crystallizing such modified RNAs are under way. This example demonstrates that one should not rely only on classic crystallization ingredients but explore alternatives as well. Modifications alter the physical properties of nucleic acids, and to obtain diffraction-quality crystals of analogs, one will often have to adapt the typical DNA crystallization conditions or even choose an innovative approach.

3.3. Hydration

A deeper understanding of how antisense modifications affect the structure and stability of nucleic acid fragments requires the assessment of modification-induced hydration changes, both at the global and the local level. Besides determining the atomic coordinates, X-ray crystallography permits the visualization of the first hydration shell as well as the thermal motion of molecular fragments and water molecules. Provided atomic-resolu-

tion diffraction data is available, molecular hydration in crystals can be assessed in great detail.[103, 115] Comparison of the hydration of the same oligonucleotide fragment in distinct crystallographic environments can reveal preserved hydration patterns, and crystallization of modified fragments in the lattice of the native molecule can indicate the differences in hydration brought about by the chemical modification.

The so-called "spine of hydration" of B-DNA dodecamers is a conserved hydration pattern that involves backbone and base atoms in the minor groove.[116, 117] Crystallization of such dodecamers with substantial incorporation of nucleotide analogs that affect the topology of the minor groove (Scheme 1, Table 1) should expose alterations in the global hydration, that is, displacements and replacements of water molecules in the spine, caused by the modifications. Similarly, crystallization of oligonucleotides with built-in single modifications allows the consequences for the local hydration to be assessed. Thus, incorporation of a 2′-*O*-methyladenosine into a DNA template provided some clues on the hydration of 2′-O-methylated riboses and its contribution to the exceptional stability of RNAs methylated at the 2′-oxygen.[106]

3.4. The Modifications

Chemical modifications of DNA and RNA affect different areas in the double helix, and Table 1 summarizes the groove locations of selected sugar and base modifications. The nucleic acid modifications thus far analyzed in our laboratory with X-ray crystallography comprise bicyclo-DNA, sulfone-RNA, carbocyclic DNA, and 2′-O-methylated RNA. The chemical alterations associated with each analog are depicted in Figure 3. Three of the modifications concern the ribose moiety, but in sulfone-RNA, the neutral dimethylene sulfone linker replaces the negatively charged phosphate group. The following sections summarize the structural findings based on single-crystal X-ray analyses for each of these nucleic acid analogs.

Table 1. Location of modifications at selected sugar and base sites in the duplex (see Figs. 1 and 2).

Modification site	Location
C2′ (sugar)	minor groove
O4′ (sugar)	minor groove
C5′ (sugar) [50]	minor groove (substituent replacing H^{Re})
C5 (base)	major groove

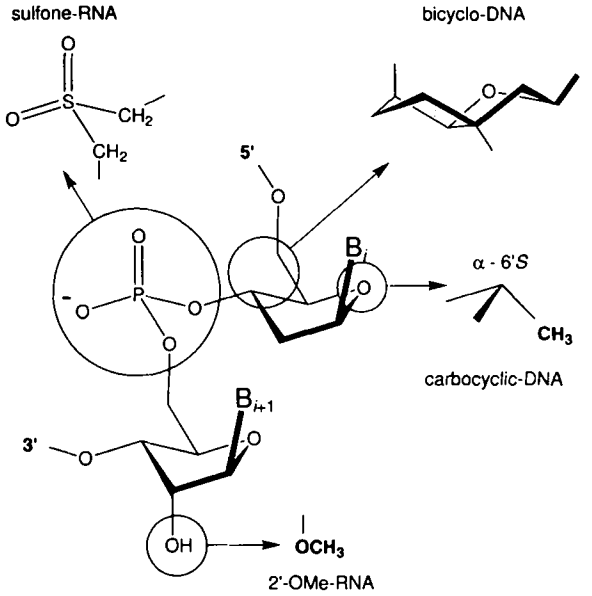

Fig. 3. Four types of DNA and RNA analogs.

4. Bicyclo-DNA

Preorganization and appropriate rigidity of the single strand are critical for the formation of stable duplexes. This was demonstrated by the drastically reduced T_m values of duplexes resulting from incorporation of open-chain glycerol building blocks into oligonucleotides,[118] as well as by the partly entropically stabilized duplexes formed by hexose-DNA.[119] Entropic stabilization of hybridization was tested in several cases. Constrained bicyclic sugar modifications include a neutral riboacetal internucleosidic linkage,[120] bicyclo-carbocyclic analogs,[121, 122] and a DNA analog with an ethylene bridge between C3′ and C5′, the so-called bicyclo-DNA (bcDNA, Fig. 3).[123] Although reduction of the entropy term upon duplex formation was achieved with the latter analogs, the affinity of the oligonucleotides containing bicyclic nucleotides for DNA and RNA was generally lower than that of the native molecules. This indicated that rigidity of the single strand alone is not sufficient for stable duplex formation, but that, in addition, the conformation adopted by the constrained nucleotide must be compatible with that of the target strand in the duplex.

The crystal structure of a bicyclic analog of the deoxycytidylyl-(3′-5′)-deoxycytidine dimer containing intranucleosidyl ethylene bridges between C3′ and C5′ (Fig. 3) was determined by X-ray diffraction at atomic resolution.[124, 125] In the crystal two bcd(CC) strands form a parallel-stranded duplex paired through hemiprotonated C–C^+ base pairs (Fig. 4). The conformations of the two single strands in the duplex deviate only minimally and, therefore, we will focus only on the conformation of the bcd(C1pC2) dimer in our discussion.

The distance between the stacked rings is 3.4 Å, and the right-handed helical twist is 34°. The paired bases display slight propeller twisting (Fig. 4, top). This arrangement leads to extensive overlap between cytosine rings within one strand, and the relative intrastrand positionings of the base carbonyl groups are likely to provide additional stability through dipole–dipole interactions (Fig. 4, bottom). The bicyclic sugars in the dimer adopt different conformations. The pucker of the C(1) deoxyribose moiety is of the C1′-*exo* type, and that of residue C(2) is of the C2′-*endo* type.

The conformations of the two cytidines also differ in their glycosidic torsion angles. Both fall into the *anti* range, but differ by about 40° (Fig. 5). Due to the conformational heterogeneity of residues in the duplex, it is impossible to build an extended parallel-stranded poly(bcdC)–poly(bcdC) duplex with continuous backbones and a single base pair as the repetitive unit.

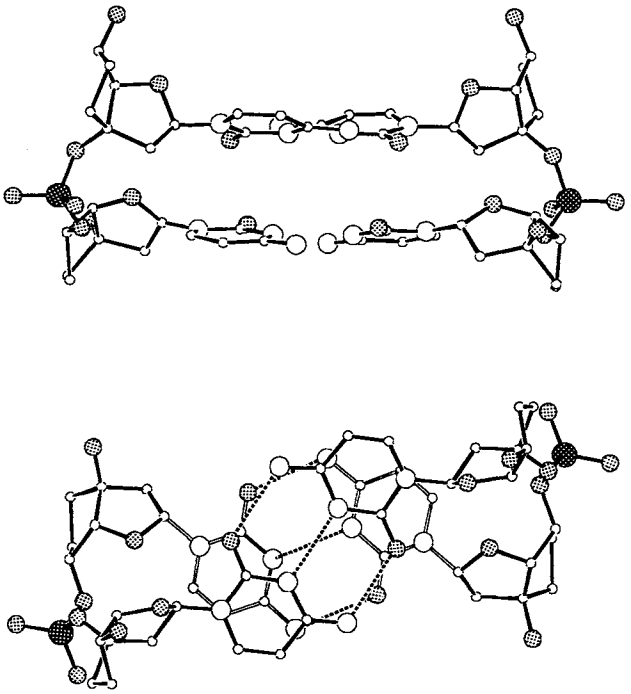

Fig. 4. The parallel-stranded [bcd(CC)]$_2$ duplex viewed along the planes of the base pairs (top), and in the direction of the helix axis (bottom). Here and in the following figures phosphorus atoms are dark gray, oxygen atoms are light gray, and hydrogen bonds are denoted by dashed lines.

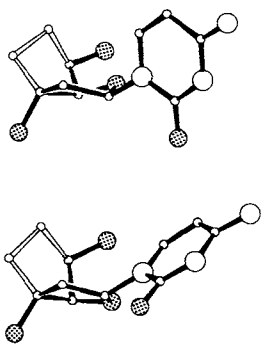

Fig. 5. Conformations of the nucleosides in bcd(CC). The deoxyribose puckers for residues C(1) and C(2) are C1′-*exo* (top) and C2′-*endo* (bottom), respectively. The ethylene bridge linking C3′ and C5′ in bcDNA is highlighted with white bonds.

In the bcDNA dimer the significant deviation from standard B-DNA geometry results in differences in the backbone torsion angles β and γ. These adopt sc^+ and *ap* conformations, respectively, in the bicyclic sugar–phosphate backbone, but are *ap* and sc^+ in B-DNA and A-RNA (where γ in an extended backbone variant can also be *ap*). The opening up of the torsion angle γ is a direct consequence of the modification in the sugar framework of bcDNA.

Cytidine-rich DNA can adopt a four-stranded arrangement composed of two interdigitated duplexes that are paired through hemiprotonated C–C$^+$ base pairs.[126] In this intercalated motif (i-motif) adjacent base pairs are about 6.2 Å apart, allowing for intercalation of base pairs from the second parallel-stranded interpenetrating duplex (Fig. 6). In this arrangement only exocyclic functions overlap, whereas the π-electron systems of the cytosine rings are not directly involved in stacking. Thus, the dipole–dipole interactions between adjacent C2=O2 carbonyl bonds and between adjacent C4–N4 bonds as well as C–H$\cdots$O4′ hydrogen bonds between more closely spaced pairs of sugar–phosphate backbones in intercalated duplexes (Fig. 6) appear to be the main stabilizing factors.[127] In the i-motif neighboring carbonyl bonds are oriented in an antiparallel fashion, while they are parallel in the [bcd(CC)]$_2$ duplex (see Figs. 4 and 6).

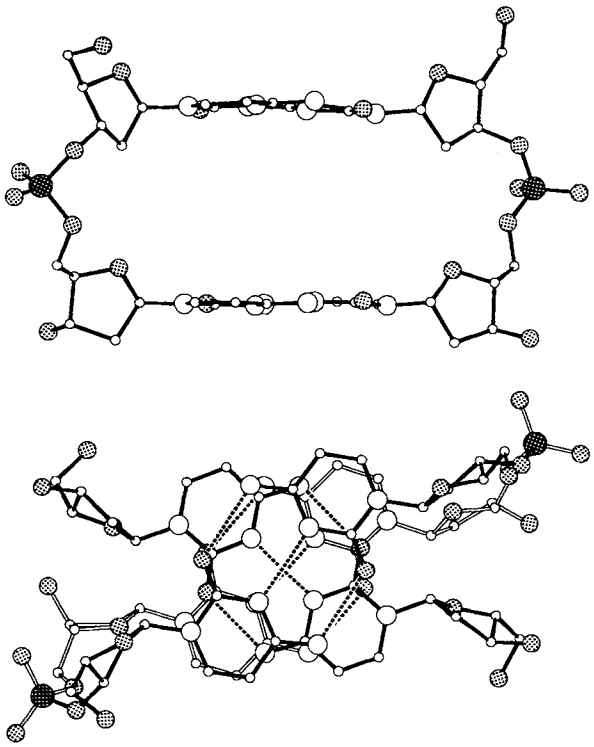

Fig. 6. The C(2)pC(3)·C(6)pC(7) base-pair step in one of the two parallel-stranded intercalated [d(CCCC)]$_2$ duplexes viewed along the planes of the base pairs (top) and in the direction of the helix axis (bottom). In the axial projection the intercalating C–C$^+$ base pair has been included and the C3–C7 base pair is highlighted with white bonds.

About half the deoxyriboses in the i-motif adopt A-type sugar puckers. The increase in the distances between adjacent base pairs in an axial direction is characterized by local changes in the backbone torsion angles. Thus, numerous α,γ pairs are found in the *ap*,*ap* range, a pattern commonly observed in the backbone region around the intercalation sites in DNA–drug complexes.[94]

The geometry of the sugar–phosphate backbone in bcDNA is different from that in B-DNA and in the i-motif. Although the ethylene bridge renders the sugar portion more rigid, the constraints introduced cause a significant deviation in strand conformation from that of a typical B-duplex and abate the entropic stability gains. To date, no diffraction-quality crystals of the native d(CC) dimer have been obtained. This may indicate that stable formation of the intercalated four-stranded motif requires a cytidine section of a minimum length. Perhaps the parallel-stranded zwitterionic bcDNA double helix constitutes an independent pairing structure that does not exist for cytidine-rich oligodeoxynucleotides.

5. Sulfone-RNA

The effect of removing the negative charge carried by phosphodiester backbones in DNA and RNA on the structure of the double helix has been relatively little studied. In duplex DNA the arrangement of negatively charged phosphates along the backbones creates a symmetric charge distribution. Disturbing this balance through neutralization of the negative charges on one face of the DNA bends the DNA toward that face.[78, 128]

With B-form DNA one can expect the degree of deformation to be more severe when the neutralization of charges concerns phosphates arranged on opposite sides of the narrow minor groove than when they flank the wide major groove.

The prospect of improved cell delivery with species that are more lipophilic than DNA and RNA has provided motivation for developing several nonionic nucleic acid analogs. Moreover, the lack of charge repulsion between phosphates in duplexes comprising an uncharged species and RNA may lead to enhanced binding stability of analogs compared with that of DNA and RNA. The methylphosphonates constitute the first uncharged nucleic acid analog. However, replacing one of the nonbridging phosphate oxygens by a methyl group leads to diastereoisomers. The dimethylene sulfone linker was conceived as a roughly isosteric, neutral, and achiral replacement for the phosphate group in DNA (Fig. 3).[55, 129] Synthetic protocols have recently been developed for the synthesis of dimethylene sulfone linked RNA.[130] The consequences of charge removal on the geometry of the RNA double helix were analyzed in the crystal structure of the dimethylene sulfone linked ribodinucleotide analog r(G-SO_2-C).[131] This crystal structure revealed that the neutral RNA analog adopts a relatively regular portion of a right-handed Watson–Crick-type double helix (Fig. 7). Overall,

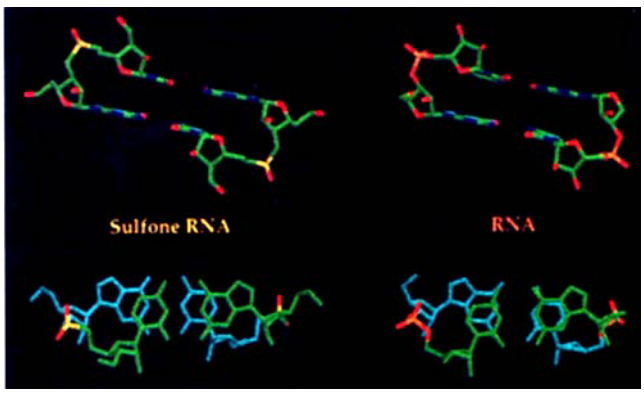

Fig. 7. The double helices formed by the nonionic dimethylene sulfone RNA analog r(G-SO_2-C) and the natural RNA dimer r(GpC) [132,133]. The images in the top half of the figure are projections into the minor groove, approximately along the crystallographic twofold rotation axes, and those in the bottom half are projections along the normal to the plane of the top base pair (green bonds). Sulfur atoms are yellow and phosphorus atoms are orange.

this duplex is quite similar to the one formed by the natural r(GpC) RNA dimer. Although the dimethylene sulfone RNA duplex appears wider at first glance, the actual S···S and P···P distances differ only by 0.3 Å. However, the backbones in the dimethylene sulfone duplex are more inclined relative to the base pair planes than those in $[r(GpC)]_2$. This is accompanied by a pronounced sliding of base pairs relative to one another in $[r(G\text{-}SO_2\text{-}C)]_2$, as well as a concomitant loss of overlap between the aromatic rings of stacked bases and a slightly decreased stacking distance in the sulfone duplex (3.4 Å vs. 3.68 Å in the phosphate duplex, Fig. 7). In addition to these changes, the helical twist in $[r(G\text{-}SO_2\text{-}C)]_2$ is about 14° less than that in $[r(GpC)]_2$, discernable by the angle between the glycosidic bonds of the guanosine and cytidine residues for both dimers (Fig. 7, bottom left and right).

Careful consideration of the possible causes of the structural perturbations in the sulfone-RNA duplex points largely to one of the methylene groups replacing the bridging phosphate ester oxygens, rather than the lack of charge. Notably, all the sugar–sulfone backbone torsion angles lie in the conformational ranges associated with an A-type duplex.[131] Both riboses adopt fairly standard C3′-*endo*-type puckers and the glycosidic bonds are in the *anti* conformation. The lack of *gauche* interactions, which are in natural nucleosides between O3′ and O4′, for 3′-CH_2-substituted (termed C3″ for sulfones) ribonucleosides would stabilize such a sugar pucker. However, the accommodation of the methylene group replacing O5′ (termed C6′ for sulfones) requires an adjustment of the nucleotide conformation (Fig. 8). Thus, the H^{Re} hydrogen of C6′ occupies roughly the position taken by O5′ in the standard phosphate backbone of A-form duplexes. This is achieved by slight changes in the sugar conformation, and in particular, by pushing the δ angle out toward 90° for a more equatorial arrangement of the C4′–C5′ and C1′–N1 bonds relative to the ribose ring. In addition, as a result of the more distinct antiperiplanar conformation of the glycosidic bond, the interaction between the H^{Re} hydrogen of C6′ and the hydrogen of C6 is minimized.

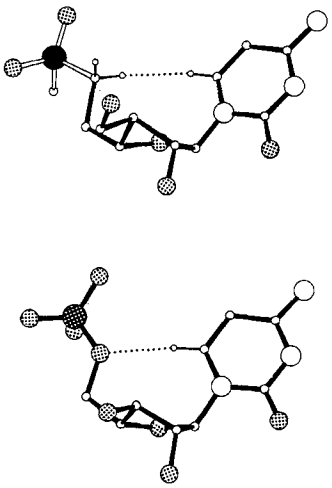

Fig. 8. The conformations of cytidine in the dimethylene sulfone RNA duplex $[r(G\text{-}SO_2\text{-}C)]_2$ (top) and in the natural $[r(GpC)]_2$ duplex (bottom). The dotted lines indicate the distances between H6 and $H6'^{Re}$ in the dimethylene sulfone duplex (2.21 Å) as well as between H6 and O5′ in the natural duplex (2.34 Å). Note the slight difference in ribose puckers in the two nucleotides. The sulfur atom is black, S=O and S–CH_2 bonds are highlighted, and the phosphorus is dark gray.

These changes in the relative positions of sugar and base together with the difference in the P–O and S–C bond lengths (the latter is approximately 0.2 Å longer) are largely responsible for the altered slide in $[r(G\text{-}SO_2\text{-}C)]_2$. Because the C6′–S bond is roughly parallel to the Watson–Crick hydrogen bonds (Fig. 7), the C6′ carbon contributes more substantially to the pronounced slide than the C3″ carbon. The lower twist in the dimethylene sulfone duplex is most likely the consequence of the difference between the S-C6′-C5′ (111°) and the P-O5′-C5′ (120°) bond angles (Fig. 7, bottom). The tighter elbow in $[r(G\text{-}SO_2\text{-}C)]_2$ rotates the green C(2)–G(3) base pair back over the blue G(1)–C(4) base pair.

The almost identical conformations of nucleosides in the dimethylene sulfone dimer allow the construction of an extended oligonucleotide duplex based on the helical twist and rise in $[r(G\text{-}SO_2\text{-}C)]_2$. A comparison between such a duplex and a standard A-RNA duplex is depicted in Figure 9. The sulfone-RNA duplex has about 17 repeats per full turn compared with the 11 repeats in standard A-RNA, and its diameter is 50% larger than that of RNA. This generates a hollow cylinder around the helix axis on the inside. The deep major groove

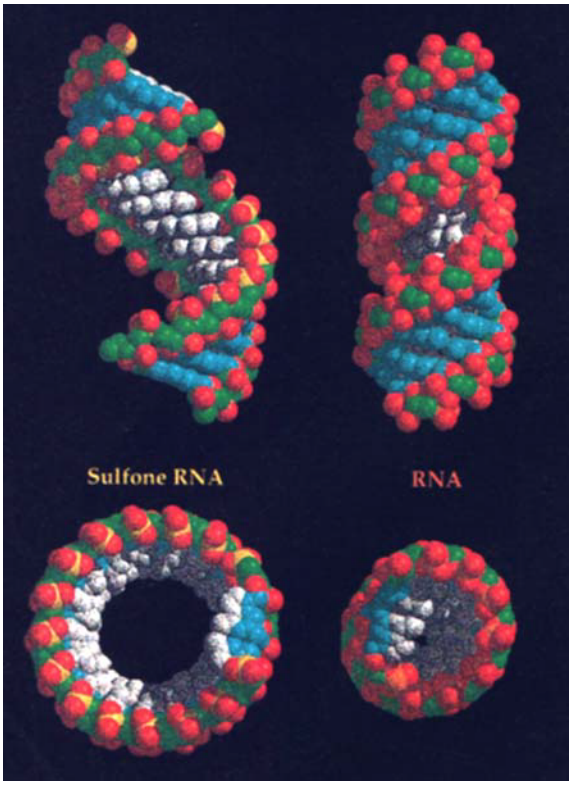

Fig. 9. Projections along the normal to the helix axis (top) and along the helix axis (bottom) of a full turn of a sulfone-RNA double helix (construction of the 17mer is based on the conformation of the $[r(G\text{-}SO_2\text{-}C)]_2$ dimer duplex) and a standard A-RNA of equal length. The edges of base pairs along the major groove are white and those along the minor groove are cyan. Sulfur atoms are yellow and phosphorus atoms are orange.

of A-RNA is opened up greatly in the sulfone duplex, and the distance separating sulfurs of opposite strands across that groove is extended to about 15 Å, or roughly three times the distance between phosphates in standard RNA. The changes in the minor groove are much less severe by comparison.

The reader should note that the rather drastic topological differences between sulfone-RNA and RNA as assessed by the structure determination of the $[r(G\text{-}SO_2\text{-}C)]_2$ duplex may represent a "worst case" scenario. The incorporation of a short stretch of sulfone-RNA into a native or otherwise modified RNA oligonucleotide may have less severe conformational consequences. Likewise, the larger slide and the smaller twist between base pairs in sulfone-RNA could lead to improved stacking beween interstrand purines in 5′-pyrimidine–purine-3′ steps and therefore higher stability. The synthesis of chimeric DNA/sulfone-DNA and RNA/sulfone-RNA oligonucleotides is under way, and it will be interesting to analyze their structures and to assess the consequences of incorporating dimethylene sulfone linked dimers into standard oligonucleotides on thermodynamic stability.

The conformational consequences of the replacement of O5′ by a methylene group have been studied with the r(UpcA) 5′-deoxy-5′-phosphonomethylene dimer,[134] and with r(A-$(pcA)_8$-pcA) 5′-deoxy-5′-phosphonomethylene-adenosine decamers.[135] For the former, circular dichroism experiments indicated that the incorporated methylene group destroyed the stacking in the dimer. However, the stability of triplexes formed by the above 5′-modified homo(A) decamer with two $r(U)_{10}$ strands was similar to that exhibited by the natural RNA oligonucleotides. The contradictory findings may be related to the different lengths and sequences of the molecules investigated. The conformational consequences of replacing O5′ by a methylene group are most likely different for purine and pyrimidine nucleosides. Thus, the methylene group may be more easily accommodated opposite H8 of adenosine than in the vicinity of H6 in cytidine as in $[r(G\text{-}SO_2\text{-}C)]_2$ (Fig. 8). Since the S–C and P–C bond lengths differ only minimally, it is unlikely that phosphonomethylene and dimethylene sulfone linkers lead to much different stacking. Further, an assumed slight loss of intrastrand stacking as observed in $[r(G\text{-}SO_2\text{-}C)]_2$ could affect the stability of double or triple helical arrangements of homopurine strands less severely (cf. the stability of the abovementioned oligo-5′-deoxy-5′-phosphonomethylene-adenosine) than that of double and triple helices composed of mixed purine–pyrimidine sequences. Recently the synthesis and incorporation in oligonucleotides of a thymidine dimer containing an internucleoside phosphinato linkage (O5′ as well as O3′ replaced by methylene groups) have been reported.[136] It is noteworthy that the hybridization of a DNA with ten consecutive phosphinate nucleotides and its RNA complement resulted in a reduction in the melting temperature of slightly less than 2 °C per modification relative to that of the native hybrid. It remains to be seen how additional replacement of the negatively charged PO_2^- portion by SO_2, as in dimethylene sulfone RNA, will affect the RNA affinity.

The crystal structure of the dimethylene sulfone linked $r(A\text{-}SO_2U)$ dimer in a single-stranded state and a comparison of its conformation to that of the $r(G\text{-}SO_2\text{-}C)$ strand in the duplex state have shed some light on the conformational rearrangements required—in this particular case—for the transformation of a single strand into a duplex.[137] The single-stranded dimer shows an extended conformation, in which all torsion angles in the sugar–sulfone backbone (except δ) adopt an *ap* conformation. Interestingly, the riboses in the $r(ASO_2U)$ dimer have C2′-*exo* puckers (Fig. 10). The *ap* conformation of γ rotates one of the C5′ hydrogens much more toward the β-face of the ribose ring. A standard C3′-*endo* conformation of the ribose as seen in the duplex would cause an unfavorable steric interaction between this C5′ hydrogen and H3′. This is avoided by folding down the C4′-C3′-C2′ elbow in the ribose (Fig. 10). Flipping α

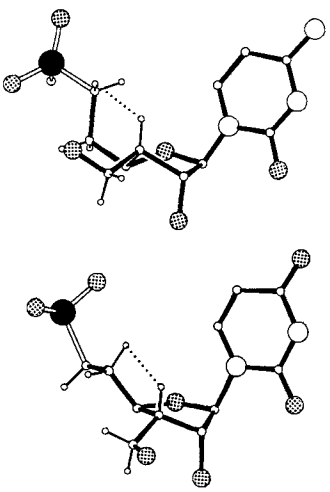

Fig. 10. C3′-*endo* pucker of cytidine in $[r(G\text{-}SO_2\text{-}C)]_2$ (top) and C2′-*exo* pucker of uridine in the $r(A\text{-}SO_2\text{-}U)$ single strand (bottom). The dotted lines mark the distances between H^{Si} of C6′ and H3′ in cytidine (2.16 Å) and between one of the C5′ hydrogens and H3′ in uridine (2.35 Å). Note the different conformations of torsion angle γ in the two nucleotides. Adoption of a C3′-*endo* pucker in uridine would generate an unfavorable interaction between H^{Re} and C5′. The sulfur atom is black.

and γ into a sc^+ conformation could allow the ribose to assume a C3′-*endo* pucker, and additional rotation around ζ would then convert the extended single-stranded conformation in r(A-SO_2-U) to a stacked arrangement similar to the one in the [r(G-SO_2-C)]$_2$ A-type duplex.

6. 6′-α-Substituted Carbocyclic DNA

In carbocyclic analogs the 4′-oxygen of the natural furanosyl nucleoside is replaced by a substituted methylene group (Fig. 3, Scheme 1). Removal of the electron-withdrawing 4′-oxygen in the furanosyl moiety has a significant effect on the basicity of the pyrimidine heterocycle. The carbocyclic analog of 5-methyl-2′-deoxycytidine has a higher pK_a than the parent compound and was shown to increase the stability of Pu·Py–Py type triple helices (requiring protonation of cytidine in the third strand).[156] In addition, the higher stability conferred by carbocyclic residues in the pyrimidine strand may be related to the absence of repulsive interactions between phosphates of the purine strand and the 4′-oxygens of the third strand bound in the major groove.[25] Carbocyclic analogs exhibit greater resistance to enzymatic cleavage of the glycosidic linkage and therefore may be useful in therapeutic applications.[138]

Although oligonucleotides containing carbocyclic building blocks showed favorable RNA-binding properties, it is believed that their stability against nuclease degradation does not suffice for biological applications.[25] Oligonucleotides containing carbocyclic analogs with α-substituents on the CH_2 group (termed C6′, Fig. 3) were found to be more resistant to degradation.[57] However, those analogs with the most significant decrease in DNA/RNA duplex stability are the very ones that show the highest degree of nuclease resistance. The experiences gathered thus far on the stability of DNA homo- and DNA/RNA heteroduplexes containing carbocyclic oligonucleotides are consistent with no particular conformational preference of the cyclopentane ring. Rather, the lack of stereoelectronic effects influencing the conformation in the furanosyl moiety render the five-membered ring much more flexible, and may allow carbocyclic nucleotides to adapt to a variety of induced duplex geometries.

In order to assess the conformational features of carbocyclic nucleotides, we incorporated three types of carbocyclic analogs, both with and without 6′-α-substituents, into a Dickerson–Drew d(CGCGAATTCGCG) template sequence (Scheme 1). Crystals could be grown of all four modified strands synthesized thus far. However, in all but one case, the crystals diffracted to relatively low resolution. To our knowledge, the rhombohedral space group of the carbocyclic dodecamer crystals has never been observed with any of the numerous variants of the dodecamer sequence crystallized during the last 15 years. More than 30 d(CGCxyyyyzGCG)-type (x = G, A, T; y = A, T; z = C, A, T) dodecamers with either sequence alterations, chemical modifications, or minor groove binding drugs complexed to them all crystallized in the orthorhombic $P2_12_12_1$ space group of the native dodecamer.[107] It is noteworthy that an apparently subtle chemical modification like the replacement of O4′ by CH_2 in a few nucleotides causes the dodecamer to pack in a different fashion, perhaps resulting in an altered conformation of the DNA.

The crystal structure of d(CGCGAAT^{Me}T^{Me}CGCG) (T^{Me} = 6′-α-methylthymidine) has been determined at 2.5 Å resolution.[139] The structure is isomorphous to that of the unmodified dodecamer, and the four modified nucleotides per duplex adopt conformations compatible with a B-DNA. Of the twenty sugar units (omitting terminal residues) in the native structure, ten have C1′-*exo*, seven have C2′-*endo*, and two have O4′-*endo* conformations, and one assumes an O4′-*exo* pucker.[140, 141] In the native structure, residues T(7) and T(8) adopt O4′-*endo* and C1′-*exo* puckers, respectively, while they display C2′-*endo* and C1′-*exo* conformations, respectively, in the modified dodecamer (Fig. 11). In the second strand, residues T(19) and T(20) in the native dodecamer both adopt C1′-*exo* puckers, while T^{Me}(19) and T^{Me}(20) in the modified duplex have C2′-*endo* and C1′-*exo* puckers, respectively. Thus, the carbocyclic residues cause only very minor deviations from the standard geometry of the deoxyoligonucleotide duplex, and the cyclopentane rings adjust smoothly to the geometrical constraints posed by the furanosyl–phosphate backbone. This may indicate that the cyclopentane ring of unsubstituted and 6′-α-substituted carbocyclic nucleotides is "conformationally promiscuous", and can comply with a range of geometries dictated by either RNA or DNA backbones.

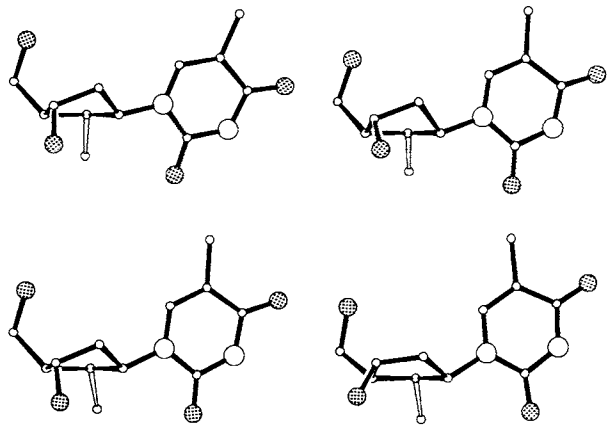

Fig. 11. Conformations of the four carbocyclic 6′-α-methylthymidines in [d(CGCGAAT^{Me}T^{Me}CGCG)]$_2$: T(8) (C2′-*endo*, top left), T(9) (C1′-*exo*, top right), T(19) (C2′-*endo*, bottom left), and T(20) (C1′-*exo*, bottom right). The C6′–C7′ bonds are highlighted.

In the central portion of the minor groove in [d(CGCGAATTCGCG)]$_2$, seven water molecules in the first hydration shell were found to link the guanine N3 or N2, adenine N3, and cytosine and thymine O2 from opposite strands, such that the bridges span two adjacent base pairs (Fig. 12, left). Six water molecules in the second hydration shell then coordinate to those of the first hydration shell with direct contacts to the DNA, thus conferring them with nearly tetrahedral coordination.[116] The ribose 4′-oxygens that line the minor groove stabilize the hydration spine, either through direct hydrogen bonds or by creating a polar environment.[117] It is surprising how little the presence of the methyl groups of the carbocyclic thymidines in the central region of the modified duplex affects the first hydration

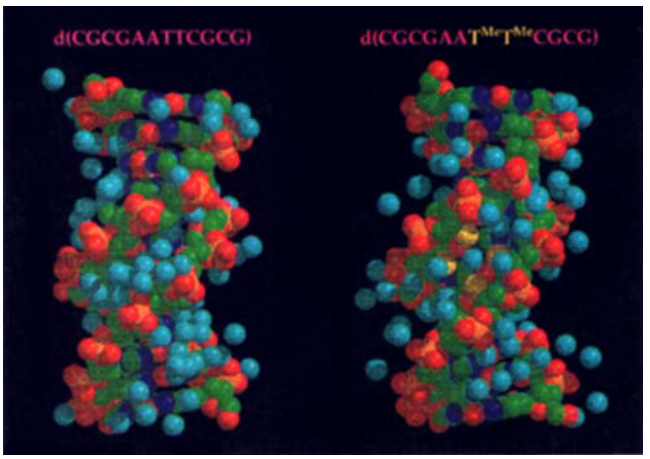

Fig. 12. Hydration of the minor groove in the B-DNA duplexes $[(d(CGCGAATTCGCG)]_2$ (left) and $[d(CGCGAAT^{Me}T^{Me}CGCG)]_2$ (right). Water molecules are represented as blue spheres and the CH_3 carbon atoms of the α-substituents in the modified thymidine residues are highlighted in yellow. The spine of hydration is visible as a chain of water molecules from the first and second hydration shell running down the minor groove in the modified duplex. The view of the central portion of the spine in the native dodecamer is slightly obstructed by water molecules of higher hydration spheres without contacts to the DNA.

shell. As in the native dodecamer, a water molecule bridges the O2 oxygens of residues $T^{Me}(7)$ and $T^{Me}(19)$. This water molecule is sealed off from the outer part of the minor groove by the four methyl groups, one of which forms a contact of 3.12 Å to the water molecule (Fig. 12, right). Two water molecules flanking the central water unit and bridging residues $T^{Me}(8)$ and A(18) as well as A(6) and $T^{Me}(20)$ are also conserved, as is the entire hydration pattern at the floor of the minor groove. However, the lipophilic patch formed by the methyl groups in the center of the minor groove leads to displacement of the water molecules of the second hydration shell that link the three water molecules in the center. In the B-DNA duplex, both the vector defined by the 6′-α-methyl carbon atoms of residues $T^{Me}(7)$ and $T^{Me}(20)$ and the vector defined by those carbons in $T^{Me}(8)$ and $T^{Me}(19)$ are roughly perpendicular to the direction of the minor groove. Thus, the distances between the methyl carbons of these residues across the groove are 1.21 and 0.87 Å, respectively (after subtraction of 4 Å, the sum of the van der Waals radii of methyl groups). The corresponding intrastrand distances between the methyl carbons of residues $T^{Me}(7)$ and $T^{Me}(8)$ and residues $T^{Me}(19)$ and $T^{Me}(20)$ are 1.03 and 0.53 Å, respectively.

The structure demonstrates that 6′-α-substituted carbocyclic nucleotides can mimic the furanosyl conformation in a duplex with B-type geometry. Insertion of isolated 6′-α-methylated building blocks into DNA could destabilize the duplex by distorting the global hydration motif. However, contiguous stretches of ten 6′-α-methylated carbocyclic pyrimidines resulted in duplexes with slightly elevated melting temperatures per incorporated residue compared with that after insertion of isolated analogs ($\Delta T_m = -1.3$ °C vs. -1.7 °C, complement DNA).[139, 142] This cooperative relative stability increase may arise from the release of water molecules in the vicinity of the methyl substituents and the near van der Waals contacts between methyl groups of adjacent intrastrand residues.

7. 2′-O-Methylated RNA

2′-O-Alkylation[40, 62, 143] and 2′-alkyl substitution[144] lead to oligonucleotides with improved metabolic stability. Heteroduplexes composed of 2′-O-alkylated RNA and natural RNA are more stable than those composed of DNA and RNA, and smaller substituents such as methyl, ethyl, and allyl are more stabilizing than longer chain alkyls.[39, 42] The 2′-hydroxyl group of RNA contributes to the thermodynamic stability of the RNA duplex, both enthalpically by improvement of hydration and entropically by conformational preorganization of the ribose.

The crystal structure of the A-RNA duplex $[r(C_4G_4)]_2$ at high resolution[103] and its comparison with the crystal structure of the A-DNA duplex with identical sequence[145, 146] have provided evidence for the superb hydration of the RNA duplex as a result of the 2′-hydroxyl groups in the minor groove (Fig. 13).

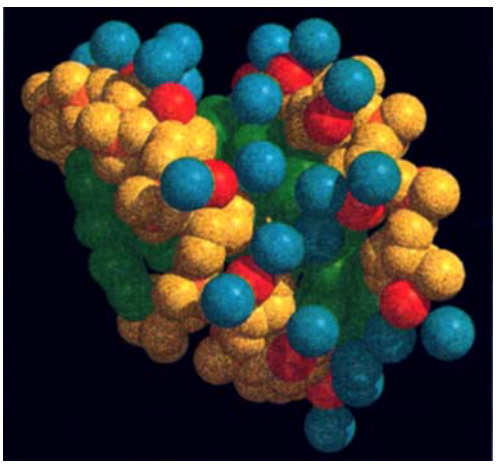

Fig. 13. Hydration of the 2′-hydroxyl groups in the minor groove of the RNA duplex $[r(C_4G_4)]_2$. Each of the water molecules (cyan, partly hidden) lies within 3.4 Å of a 2′-oxygen (red). Phosphorus atoms are orange, the remaining atoms in the ribose–phosphate backbone are yellow, and base atoms are green.

They form hydrogen bonds to two water molecules on average, and most of them serve as donors in an additional internal hydrogen bond to the 4′-oxygen of the adjacent ribose in the 5′ → 3′ direction.

The thermodynamics of hybridization for $r(C_4G_4)$ and $d(C_4G_4)$ were calculated from temperature-dependent UV-spectroscopic data. Perhaps surprisingly, the higher thermodynamic stability of the RNA duplex compared with that of the DNA duplex is not based on a more favorable entropy term, which would be a consequence of the conformational preorganization of the ribose–phosphate backbone in single-stranded RNA for an A-form duplex. Instead, the enthalpy for duplex formation for RNA is more than 30 kcal mol^{-1} higher than for DNA, consistent with the much better hydration of the RNA observed in the crystal (see 2′-OH hydration in Fig. 13). DNA duplex formation may cause a net loss of water molecules, whereas the overall number of water molecules may not be too different in the case of two RNA single strands and an RNA duplex. The very minor loss of hydration (or perhaps even slight increase) for RNA upon duplexation (entropically unfavorable) opposes

Table 2. Thermodynamic data for $r(C_4G_4)$ and $d(C_4G_4)$ based on temperature-dependent UV-hyperchromicity measurements [a].

Oligomer	T_m [°C]	ΔG [kcal mol^{-1}]	ΔH [kcal mol^{-1}]	$-T\cdot\Delta S$ [kcal mol^{-1}]
$d(C_4G_4)$	44.6	−8.4	−54.0	+45.6
$r(C_4G_4)$	70.1	−15.5	−85.1	+69.6

[a] The T_m values were measured in 10 mM sodium cacodylate (pH 7), 100 mM NaCl, 0.1 mM EDTA, at strand concentrations of 8.2 μM. Thermodynamic data are given for 37 °C.

the enthalpy gains due to bound water as well as the contribution from the preorganization of the single strand, which should favorably influence the entropy term. Nevertheless, the gains in enthalpy are higher than the losses in entropy, and the ΔG for duplex formation with RNA is roughly twice that of duplex formation with DNA (Table 2). It is interesting in this context that oligonucleotides containing 2′-alkoxy-substituted carbocyclic building blocks lacking the *gauche* interaction between the 2′-substituent and the 4′-ribose oxygen show reduced RNA-binding affinity relative to that of the corresponding DNA oligonucleotides.[57] Thus, the greater rigidity of RNA relative to DNA due to the *gauche* interaction between O2′ and O4′ in the sugar–phosphate backbone and the resulting entropic advantage for duplex formation are of crucial importance for the higher thermodynamic stability of RNA and 2′-*O*-Me-RNA.

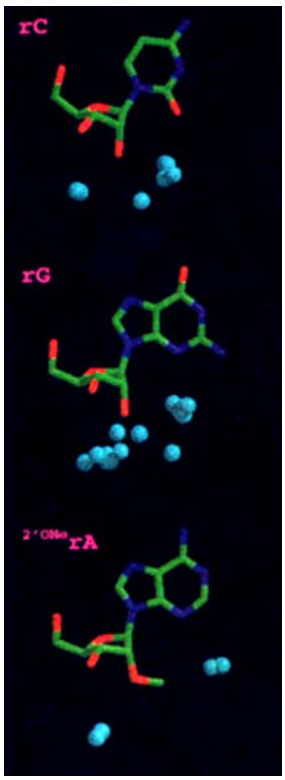

Fig. 14. Consensus hydration pattern of the minor groove in the vicinity of rC (top), rG (middle), and 2′-*O*-Me-rA (bottom). To generate each of the rC and rG pictures, the appropriate eight nucleosides in the $[r(C_4G_4)]_2$ crystal structure (replaced here with a nucleoside with a consensus conformation) and the water molecules around them were superimposed. The hydration pattern of $^{2'OMe}$rA is based on the hydration of the two modified adenosines observed in the crystal structure of a chimeric DNA:2′-*O*-Me RNA decamer duplex [106].

In the crystal structure of the decamer duplex $[d(GCGT)^{O2'Me}r(A)d(TACGC)]_2$, which contains 2′-*O*-methylated adenosines, both methoxy oxygens form a hydrogen bond to only one water molecule.[106] Thus, methylation of the 2′-hydroxyl group leads to a reduced hydration compared with that of native RNA (where 2′-hydroxyl groups are most often bound to two water molecules), and, in addition, disrupts the internal hydrogen bond often observed between O2′ and O4′ of the adjacent intrastrand ribose. The consensus patterns of minor groove hydration for cytidine and guanosine based on the $[r(C_4G_4)]_2$ crystal structure are depicted in the upper portion of Figure 14. There, the 2′-hydroxyl groups stabilize a continous band of water molecules across the groove, which are arranged more or less within the planes defined by the G–C base pairs and link backbones and bases (Fig. 13, foreground). For most of the G–C base pairs, one of the two water molecules hydrogen bonded to the 2′-oxygen atoms is located at the border of the minor groove and forms a bridge between O2′ and the phosphate group. The other water molecule then links O2′ to N3 of guanosine or to O2 of cytidine (Fig. 14). These water molecules are in turn bridged by a fifth water, which normally also forms a hydrogen bond to N2 of guanosine (not included in Fig. 13, as these water molecules do not interact directly with 2′-oxygens).

In the arrangement of water molecules around 2′-O-methylated adenosines it is apparent that the water molecule formerly linking O2′ to N3 (in analogy to G in the RNA duplex) is shifted to the center of the groove by the methoxy group (Fig. 14, bottom). Both the crystal structure and solution NMR experiments[71] provide evidence that the methoxy substituents point into the minor groove, resulting in an approximate *trans* conformation of the C2′–C3′ and O2′–CH_3 bonds. Accordingly, 2′-O-methylation of RNA seems to distort minor groove hydration at the local and the global level, suggesting that the superior stability of 2′-*O*-Me RNA could be mainly entropy driven. This is supported by the even higher thermodynamic stability of hybrids formed between 2′-deoxy-2′-fluorooligonucleotides and RNA.[42, 147] Although hydrogen bonding to covalently bound fluorine atoms has been invoked,[148] fluorine (in contrast to the fluoride anion) is an extremely poor hydrogen bond acceptor.[149] The strong RNA affinity of oligodeoxynucleotides with uniform 2′-fluoro substitution is therefore unlikely to be accounted for by enthalpic stabilization through hydration. However, electronegativity effects that stabilize the C3′-*endo* sugar pucker provide an important contribution to the exceptional RNA affinity.[99] Taken together, the structural and thermodynamic data support the view that 2′-*O*-Me RNA may combine an entropic stabilization similar to that of DNA through loss of water upon duplex formation with the entropic stabilization of RNA through conformational preorganization of the single strand. Additional stability may be provided through hydrophobic contacts between closely spaced O2′-substituents along the strand.[106] Subtle tuning between the gain in entropy and the loss in enthalpy as a consequence of altering the hydration may well be involved in the highly stabilizing effects of a methyl group at C5 in pyrimidines[150] and the exceptional RNA affinity of oligonucleotides comprising pyrimidines with propyne substituents at the C5 position.[62]

8. Sequence-Specific Cleavage of RNA

Hetero duplexes composed of RNA and almost all oligonucleotide analogs with modified sugar and/or phosphate moieties fail to activate the natural mRNA degradation pathway mediated by RNase H. The enzyme cleaves the RNA strand in DNA·RNA hybrids, and the only analogs that do not prevent recognition of the hetero substrate by the enzyme are phosphorothioates, phosphorodithioates, and those with base modifications affecting the major groove (for example 5-propynepyrimidines).[24] This failure to induce RNA degradation may con-

stitute a serious limitation for the therapeutic application of antisense compounds. Functionalized RNAs that can recognize a specific mRNA region and efficiently cleave it,[151] as well as unmodified and chemically modified hammerhead-type ribozymes[13, 41, 152, 153] may prove more potent as antisense therapeutics.

In the ribozyme-catalyzed cleavage of RNA through transesterification of phosphodiesters, the backbone is preoriented for an S_N2-type displacement. Thus, the incoming 2′-OH group and 5′-OH leaving group must both occupy apical positions in the trigonal-bipyramidal transition state formed by the nucleophile and the phosphate group with the scissile P–O5′ bond.[154–156] In an intact A-RNA duplex, the relative positions of the 2′-OH and the adjacent 5′-phosphate group preclude an in-line attack. However, distortions in the backbone geometry around single- or multiple-base bulges appear to provide the conformational freedom necessary for efficient strand cleavage. Quantitative cleavage of an RNA strand was observed at the phosphate adjacent to a "bulged" or unpaired nucleotide in the presence of moderate amounts of Mg^{2+}.[157] The products that result from cutting the 3′-5′-phosphodiester bond between the bulged and adjacent nucleotides in a 5′ → 3′ direction are a cyclic 2′,3′-phosphodiester and a free 5′-hydroxyl group, exactly the same products obtained in the cleavage reaction catalyzed by hammerhead-type ribozymes.[158]

We have determined the crystal structure of a self-complementary RNA–DNA chimera with single adenosine bulges at a resolution of 2.8 Å (Fig. 15).[160] In the crystal the fragment adopts crystallographic twofold symmetry and both adenosines extrude from the duplex (Fig. 16). The deoxyriboses of the bulged nucleotides A(8) and A(19) as well as A(6), T(7), A(17), and A(18) adopt C2′-*endo* puckers, while all others display the C3′-*endo* conformation of A-RNA. The backbone perturbations brought about by the unpaired adenosines kink the fragment by 20° and cause a drastic opening of the narrow major groove to about twice its normal width.

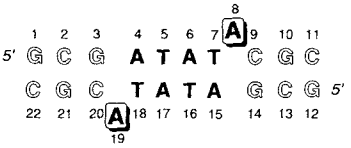

Fig. 15. Sequence of the self-complementary RNA–DNA chimera (units of RNA in outlined letters, those of DNA in filled letters) having two bulged (unpaired) adenosine residues, which was studied by X-ray crystallography. The central portion of the 11mer was originally left as DNA in order to conserve some features of a fully base-paired RNA–DNA chimera that had previously yielded high-resolution crystals [159], and to prevent strand cleavage between residues A(8) and C(9) (or A(19) and C(20)) during attempted crystallization in the presence of divalent metal cations.

In molecular modeling studies based on the crystal structure of this RNA–DNA chimera, a 2′-OH group was introduced at the deoxyribose of the bulged adenosine. As can be seen in Figure 17 (bottom), this hydroxyl group is relatively far removed from the scissile P–O5′ bond (O2′–P 4.2 Å). In addition, it lies approximately within the plane defined by the phosphate oxygens O1P, O2P, and O3′. Thus, the hypothetical O2′-P-O5′ angle of 90° would disfavor cleavage of the phosphodiester bond (Fig. 17, bottom). However, if the C2′-*endo* conformation at the ribose of the bulge residue is flipped into a C3′-*endo* pucker,

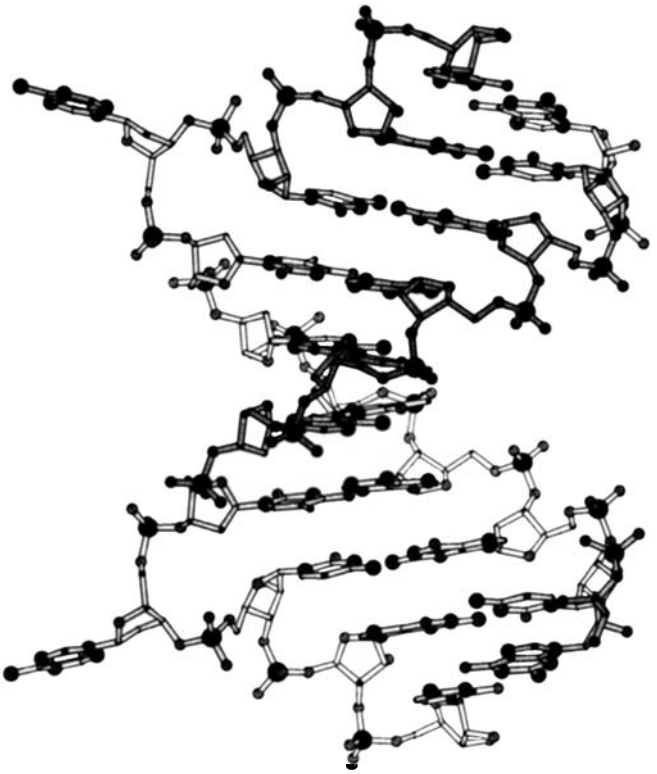

Fig. 16. Overall conformation of the A-RNA-like duplex containing bulged adenosines. Phosphorus atoms are filled circles and darker portions are closer to the viewer. Bulged adenosines are important RNA secondary structure elements and are involved in RNA folding, protein–RNA interactions, and splicing of group I and II introns as well as nuclear pre-mRNA [161–165].

a roughly apical arrangement of the 2′-OH results (O2′-P 3.6 Å, O2′-P-O5′ 150°; Fig. 17, top). This demonstrates that apical positions of incoming and leaving groups at the trigonal-bipyramidal intermediate can be achieved relatively easily as a result of local conformational rearrangements of the backbone around the bulged nucleotide, and is consistent with the efficient metal-assisted cleavage at such sites. The P-$O^{Si}\cdots O^{Re}$-P distance of 3.95 Å for residues C(9) and G(10) adjacent to the bulged nucleotide in the 5′-direction in the crystal structure is the shortest one in the entire duplex, and lies well below the usual intrastrand phosphate–phosphate contacts in A-type duplexes (Fig. 17). These closely spaced phosphate groups may provide a binding site for a Mg^{2+} ion that could activate the phosphate group for the nucleophilic attack and stabilize the 5′-hydroxyl leaving group. It is interesting that in the structure of a second crystal form, determined at a resolution of 1.83 Å,[160] the RNA–DNA chimeric fragment displays a conformation in the region of the bulged nucleotide that is very similar to the one in the modeled structure. In this structure the sugar of the bulged adenosine adopts a C3′-*endo* conformation and the added 2′-OH group assumes a nearly apical orientation relative to the phosphate group (O2′–P 3.8 Å, O2′-P-O5′ 145°).

9. Summary and Outlook

Progress in understanding of nucleic acid structure has always been intimately linked to the advances in the chemical synthesis of DNA and RNA. When milligram amounts of highly pure

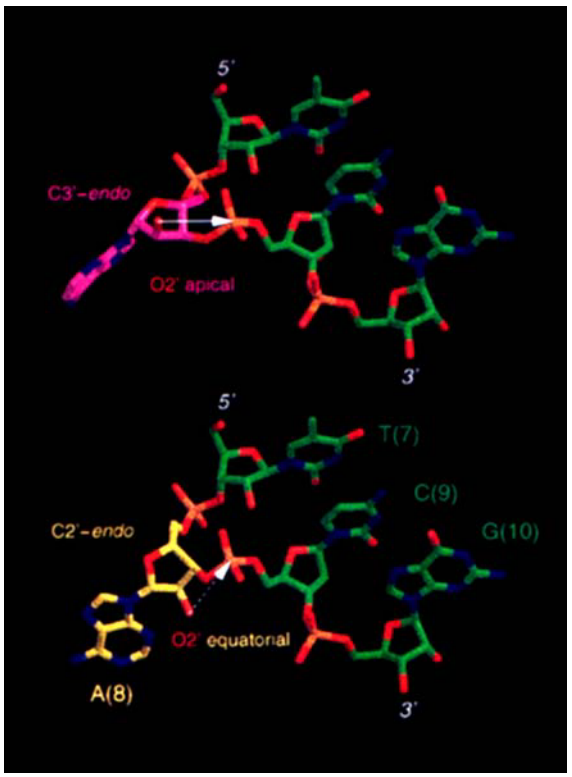

Fig. 17. Backbone conformation around the adenosine bulge (yellow) as observed in the crystal structure (bottom). Modeled backbone conformation around the adenosine bulge (purple) by changing the conformation of the sugar pucker from C2'-*endo* to C3'-*endo* (top). Solid and dashed arrows indicate the vectors between the adenosine 2'-OH, which is depicted here but missing from the crystal structure, and the phosphorus of the 3'-phosphate. The short distance between the phosphate oxygens O^{Si} and O^{Re} of residues C(9) and G(10), respectively, is visible in the foreground.

oligodeoxynucleotides became available in the early eighties, the way was paved for the first high-resolution crystal structures of DNA fragments. In somewhat more than a decade over a hundred crystal structures have given insight into many structural aspects of the double helix. Similar success with RNA has long been hampered by the difficulties encountered in developing synthesis protocols for the large-scale production of oligoribonucleotides. These have now largely been overcome and a dramatic rise in the number of RNA structures in the next years is foreseeable.

The challenge of advancing the antisense technique beyond its use as a research tool toward therapeutic applications has catalyzed the generation of an astounding variety of synthetic nucleic acid analogs. Many of them show improved resistance to cellular nuclease degradation over that of their natural counterparts. Several analogs combine higher chemical stability with increased RNA affinity.[51, 62, 166] However, with very few exceptions, such as the first-generation phosphorothioate analogs, modifications block the natural mRNA degradation pathway based on RNase H. Modified oligonucleotides that form stable complexes with newly transcribed RNA at nuclear sites and do not prevent recruitment of RNase H appear to be particularly effective in shutting down mRNA translation.[167]

Detailed three-dimensional structures provide clues to the origins of the changes in thermodynamic stability incurred by chemical modifications of DNA and RNA. A comparison of the high-resolution crystal structures of a DNA octamer and an RNA octamer duplex with identical sequences illustrates that double-helical DNA and RNA differ fundamentally in their degrees of hydration; the RNA duplex is more extensively hydrated as a result of the additional ribose 2'-hydroxyl groups. Consequently, with respect to bound H_2O, RNA duplex formation is favored enthalpically but disfavored entropically relative to DNA duplexation. The higher rigidity of the ribose moiety contributes positively to the overall thermodynamic stability of the RNA duplex. Hydration changes and the ensuing trade-off between enthalpy and entropy are mostly overlooked in the analysis of the thermodynamic stability data of nucleic acid analogs.[127] Because hydration makes an important contribution to the relative stabilities of native DNA and RNA, it would seem that changes in the solvation as a consequence of chemical modifications are a crucial factor in the altered thermodynamic stability of DNA and RNA analogs. This view is supported by the changes in hydration evident in the crystal structures of derivatives formed by introduction of methyl groups at the 2'-oxygen (2'-*O*-Me-RNA) and the 6'-carbon (carbocyclic DNA). Somewhat simplified, these results point to an equilibration or occasional overcompensation (2'-O-substituted RNA) of the enthalpy losses caused by the altered or reduced hydration in the vicinity of short-chain alkyl groups or heteroatom substituents by the entropy gains due to water loss. The close spacing of such substituents in the minor groove of the A-form duplex is likely to stabilize duplex formation, while longer chain alkyl groups, or in general bulky lipophilic substituents, disrupt hydration in such a way that the enthalpy loss becomes dominant. Hydration effects are probably also involved in the stabilization exerted by substituents at pyrimidine C5 (for example methyl or propyne); stacking and interactions between substituents provide additional contributions.

In addition to providing feedback for the design of further nucleic acid analogs for antisense applications, systematic study of the structures of chemically modified nucleic acids promises deeper insight into the properties of the native DNA and RNA molecules. Just as point mutations with proteins in combination with structural work have permitted the assessment of the individual influences of amino acids in folding and catalysis, specifically modified nucleic acids allow one to analyze the importance of various parameters for the overall structures of DNA and RNA. Thus, analogs may be helpful for an improved understanding of bending, interactions between proteins and nucleic acids, and a variety of other issues.

I wish to thank my collaborators in our laboratory, P. Lubini, S. Portmann, A. Roughton, and C. Richert, as well as those from outside institutions, C. Leumann (University of Berne), K.-H. Altmann, M. Blommers, D. Hüsken, and H. Moser (CIBA, Basel), N. Usman (Ribozyme Pharmaceuticals Inc., Boulder, USA), and F. K. Winkler (Hoffmann LaRoche, Basel) for their contributions and stimulating discussions. I am grateful to A. Roughton for his comments on the manuscript, and I would like to thank the ETH Zürich, the Organic Chemistry Laboratory, The Ciba-Geigy-Jubiläums-Stiftung, and CIBA for their financial support.

Received: July 19, 1995 [A 1231E]
German version: *Angew. Chem.* **1996**, *108*, 2020–2036

[1] P. J. Green, O. Pines, M. Inouye, *Annu. Rev. Biochem.* **1986**, *55*, 569–597.
[2] R. W. Simons, N. Kleckner, *Annu. Rev. Genet.* **1988**, *22*, 567.
[3] H. M. Weintraub, *Sci. Am.* **1990**, *262(1)*, 34–40.
[4] Y. Eguchi, T. Itoh, J. Tomizawa, *Annu. Rev. Biochem.* **1991**, *60*, 631–652.
[5] J. Tomizawa, *Cell* **1984**, *38*, 861–870.
[6] J. P. Marino, R. S. Gregorian, Jr., G. Csankovszki, D. M. Crothers, *Science* **1995**, *268*, 1448–1454.
[7] P. C. Zamecnik, M. L. Stephenson, *Proc. Natl. Acad. Sci. U. S. A.* **1978**, *75*, 280–284.
[8] M. L. Stephenson, P. C. Zamecnik, *ibid.* **1978**, *75*, 285–288.
[9] H. E. Moser, P. B. Dervan, *Science* **1987**, *238*, 645–650.
[10] T. Le Doan, L. Perronault, D. Praseuth, N. Habhoub, J. L. Decout, N. T. Thuong, J. L. Homme, C. Hélène, *Nucleic Acids Res.* **1987**, *15*, 7749–7760.
[11] J.-S. Sun, C. Hélène, *Curr. Opin. Struct. Biol.* **1993**, *3*, 345–356; N. T. Thuong, C. Hélène, *Angew. Chem.* **1993**, *105*, 697–723; *Angew. Chem. Int. Ed. Engl.* **1993**, *32*, 666–690.
[12] G. A. Prody, J. T. Bakos, J. M. Buzayan, I. R. Schneider, G. Bruening, *Science* **1986**, *231*, 1577–1580; A. C. Forster, R. H. Symons, *Cell* **1987**, *49*, 211–220; O. C. Uhlenbeck, *Nature* **1987**, *328*, 596–600.
[13] T. R. Cech, *Curr. Opin. Struct. Biol.* **1992**, *2*, 605–609; N. Usman, J. McSniggen, *Ann. Rep. Med. Chem.* **1995**, *30*, 285–294.
[14] C. A. Stein, J. S. Cohen, *Cancer Res.* **1988**, *48*, 2659–2668.
[15] J. Goodchild, *Bioconj. Chem.* **1990**, *1*, 165–187.
[16] C. Hélène, J.-J. Toulmé, *Biochim. Biophys. Acta* **1990**, *1049*, 99–125.
[17] E. Uhlmann, A. Peyman, *Chem. Rev.* **1990**, *90*, 543–584.
[18] P. Cook, *Anti-Cancer Drug Design* **1991**, *6*, 585.
[19] C. Hélène, *Anti-Cancer Drug Design* **1991**, *6*, 569–584.
[20] J. A. H. Murray, *Antisense RNA and DNA, Modern Cell Biology, Vol. 11*, Wiley-Liss, New York, **1992**.
[21] S. T. Crooke, *Curr. Opinion Biotechn.* **1992**, *3*, 656–661.
[22] R. Tullis, E. Wilkinson, J. Caravaca-Trujillo, *Biotechn. Int.* **1992**, 79–89.
[23] *Antisense Research and Applications* (Eds.: S. T. Crooke, B. Lebleu), CRC Press, Boca Raton, FL, **1993**.
[24] J. F. Milligan, M. D. Matteucci, J. C. Martin, *J. Med. Chem.* **1993**, 36, 1923–1937.
[25] H. E. Moser in *Perspectives in Medicinal Chemistry* (Eds.: B. Testa, W. Furrer, E. Kyburz, R. Giger), Helvetica Chimica Acta, Basel, **1993**, pp. 275–297, and references therein.
[26] E. Uhlmann, A. Peyman in *Methods in Molecular Biology* (Ed.: S. Agrawal), Humana, Clifton, NJ, **1993**, pp. 355–390.
[27] R. S. Varma, *Synlett* **1993**, 621–637.
[28] J. S. Cohen, M. E. Hogan, *Sci. Am.* **1994**, *Dec.*, 50–55.
[29] *Modified Oligonucleotides* (Ed.: G. L. Trainor), *Bioorg. Med. Chem. Lett.* **1994**, *4*, 965–1085.
[30] M. Z. Ratajczak, A. M. Gewirtz in *Nucleic Acids and Molecular Biology, Vol. 8* (Eds.: F. Eckstein, D. M. J. Lilley) Springer, Berlin, **1994**, pp. 298–326.
[31] R. W. Wagner, *Science* **1994**, *372*, 333–335.
[32] „Carbohydrate Modifications in Antisense Research": *ACS Symp. Ser.* **1994**, *580*.
[33] A. De Mesmaeker, K.-H. Altmann, A. Waldner, S. Wendeborn, *Curr. Opin. Struct. Biol.* **1995**, *5*, 343–355.
[34] J. A. Walder, *Biotechn. Int.* **1992**, 67–71.
[35] F. Eckstein, *Ann. Rev. Biochem.* **1986**, *54*, 367–402.
[36] G. Zon, *Biotechn. Int.* **1992**, 119–124.
[37] K. K. Chacko, K. Lindner, W. Saenger, P. S. Miller, *Nucleic Acids Res.* **1983**, *11*, 2801–2814.
[38] P. S. Miller, C. H. Agris, L. Aurelian, K. R. Blake, A. Murakami, M. P. Reddy, S. A. Spitz, P. O. P. Ts'o, *Biochimie* **1985**, *67*, 769–776.
[39] H. Inoue, Y. Hayase, A. Imura, S. Iwai, K. Miura, E. Ohtsuka, *Nucleic Acids Res.* **1987**, *15*, 6131–6148.
[40] A. M. Ibarren, B. S. Sproat, P. Neuner, I. Sulston, U. Ryder, A. I. Lamond, *Proc. Natl. Acad. Sci. USA* **1990**, 87, 7747–7751.
[41] J. Goodchild, *Nucleic Acids Res.* **1992**, *20*, 4607–4612, and references therein.
[42] E. A. Lesnik, C. J. Guinosso, A. M. Kawasaki, H. Sasmor, M. Zounes, L. L. Cummins, D. J. Ecker, P. D. Cook, S. M. Freier, *Biochemistry* **1993**, *32*, 7832–7838.
[43] X. Cao, M. D. Matteucci, *Tetrahedron Lett.* **1994**, *35*, 2325–2328.
[44] A. De Mesmaeker, J. Lebreton, A. Waldner, V. Fritsch, R. M. Wolf, S. M. Freier, *Synlett* **1993**, 733–736.
[45] C. V. C. Prasad, T. J. Caulfield, C. P. Prouty, A. K. Saha, W. C. Schairer, A. Yawman, D. A. Upson, L. I. Kruse, *Biorg. Med. Chem. Lett.* **1995**, *5*, 411–414.
[46] J. Lebreton, A. De Mesmaeker, A. Waldner, *Synlett* **1994**, 54–56.
[47] R. J. Jones, K.-Y. Lin, J. F. Milligan, S. Wadwani, M. D. Matteucci, *J. Org. Chem.* **1993**, *58*, 2983–2991.
[48] K.-I. Lin, J. S. Pudlo, R. J. Jones, N. Bischofberger, M. D. Matteucci, B. Fröhler, *Bioorg. Med. Chem. Lett.* **1994**, *4*, 1061–1064.
[49] a) R. O. Dempcy, K. A. Browne, T. C. Bruice, *J. Am. Chem. Soc.* **1995**, *117*, 6140–6141; b) R. O. Dempcy, K. A. Browne, T. C. Bruice, *Proc. Natl. Acad. Sci. USA* **1995**, *92*, 6097–6101.
[50] a) A. K. Saha, T. J. Caulfield, C. Hobbs, D. A. Upson, C. Waychunas, A. M. Yawman, *J. Org. Chem.* **1995**, *60*, 788–789; b) L. Beigelman, A. Karpeisky, N. Usman, *Nucleosides Nucleotides* **1995**, *14*, 901–905.
[51] a) S. M. Gryaznov, D. H. Lloyd, J.-K. Chen, R. G. Schultz, L. A. DeDionisio, L. Ratmeyer, W. D. Wilson, *Proc. Natl. Acad. Sci. USA* **1995**, *92*, 5798–5802; b) J.-K. Chen, R. G. Schultz, D. H. Lloyd, S. M. Gryaznov, *Nucleic Acids Res.* **1995**, *23*, 2661–2668.
[52] W. S. Marshall, M. H. Caruthers, *Science* **1993**, *259*, 1564–1570.
[53] B. Meng, S. H. Kawai, D. Wang, G. Just, P. A. Giannaris, M. J. Dahma, *Angew. Chem.* **1993**, *105*, 733–735; *Angew. Chem. Int. Ed. Engl.* **1993**, *32*, 729–731.
[54] E. B. McElroy, R. Bandaru, J. Huang, T. S. Widlanski, *Bioorg. Med. Chem. Lett.* **1994**, *4*, 1071–1076.
[55] Z. Huang, K. C. Schneider, S. A. Benner, *J. Org. Chem.* **1991**, *56*, 3869–3882.
[56] B. C. Froehler, D. J. Ricca, *J. Am. Chem. Soc.* **1992**, *114*, 8320–8322.
[57] K.-H. Altmann, M.-O. Bévierre, A. De Mesmaeker, H. E. Moser, *Biorg. Med. Chem. Lett.* **1995**, *5*, 431–436.
[58] A. Garbesi, M. L. Capobianco, F. P. Colonna, L. Tondelli, F. Acramone, G. Manzini, C. W. Hilbers, J. M. E. Aelen, M. J. J. Blommers, *Nucleic Acids Res.* **1993**, *21*, 4159–4165.
[59] A. Eschenmoser, E. Loewenthal, *Chem. Soc. Rev.* **1992**, 1–16.
[60] A. Eschenmoser in *Proceedings of the Robert A. Welch Foundation, Vol. 37*, The Robert A. Welch Foundation, Houston, TX, **1993**, pp. 201–235.
[61] P. Herdewijn, H. De Winter, B. Doboszewski, I. Verheggen, K. Augustyns, C. Hendrix, T. Saison-Behmoaras, C. De Ranter, A. Van Aerschot in ref. [32], pp. 80–99.
[62] R. W. Wagner, M. D. Matteucci, J. G. Lewis, A. J. Gutierrez, C. Moulds, B. C. Froehler, *Science* **1993**, *260*, 1510–1513.
[63] P. E. Nielsen, M. Egholm, O. Buchardt, *Bioconj. Chem.* **1994**, *5*, 3–7.
[64] A. De Mesmaeker, A. Waldner, J. Lebreton, P. Hoffmann, V. Fritsch, R. M. Wolf, S. M. Freier, *Angew Chem.* **1994**, *106*, 237–240; *Angew. Chem. Int. Ed. Engl.* **1994**, *33*, 226–229.
[65] V. Fritsch, A. De Mesmaeker, A. Waldner, J. Lebreton, M. J. J. Blommers, R. M. Wolf, *Bioorg. Med. Chem.* **1995**, *3*, 321–335.
[66] X. Gao, F. K. Brown, P. Jeffs, N. Bischofberger, K.-Y. Lin, A. J. Pipe, S. A. Noble, *Biochemistry* **1992**, *31*, 6228–6236.
[67] J. M. Veal, F. K. Brown, *J. Am. Chem. Soc.* **1995**, *117*, 1873–1880.
[68] X. Gao, P. W. Jeffs, *J. Biomol. NMR* **1994**, *4*, 17–34.
[69] A. Waldner, A. De Mesmaeker, J. Lebreton, V. Fritsch, R. M. Wolf, *Synlett* **1994**, 57–61.
[70] Y. Cho, F. C. Zhu, B. A. Luxon, D. G. Gorenstein, *J. Biomol. Struct. Dyn.* **1993**, *11*, 685–701.
[71] M. J. J. Blommers, U. Pieles, A. De Mesmaeker, *Nucleic Acids Res.* **1994**, *22*, 4187–4194.
[72] H. Robinson, K.-E. Jung, C. Switzer, A. H.-J. Wang, *J. Am. Chem. Soc.* **1995**, *117*, 837–838.
[73] S. C. Brown, S. A. Thomson, J. M. Veal, D. G. Davis, *Science* **1994**, *265*, 777–780.
[74] M. Leijon, A. Gräslund, P. E. Nielsen, O. Buchardt, B. Nordén, S. M. Kristensen, M. Eriksson, *Biochemistry* **1994**, *33*, 9820–9825.
[75] L. Betts, J. A. Josey, J. M. Veal, S. R. Jordan, *Science* **1995**, *270*, 1838–1841.
[76] R. H. Griffey, E. Lesnik, S. Freier, Y. S. Sanghvi, K. Teng, A. Kawasaki, C. Guinosso, P. Wheeler, V. Mohan, P. D. Cook in ref. [32], pp. 212–224.
[77] B. Honig, A. Nicholls, *Science* **1995**, *268*, 1144–1149, and references therein.
[78] J. K. Strauss, L. J. Maher III, *Science* **1994**, *266*, 1829–1834.
[79] K. Ezaz-Nikpay, G. L. Verdine, *Chem. Biol.* **1994**, *1*, 235–240.
[80] S. A. Wolfe, A. E. Ferentz, V. Grantcharova, M. E. A. Churchill, G. L. Verdine, *Chem. Biol.* **1995**, *2*, 213–221.
[81] J. R. Wyatt, I. Tinoco, Jr. in *The RNA World* (Hrsg.: R. F. Gesteland, J. F. Atkins), Cold Spring Harbor Laboratory Press, Cold Spring Harbor, NY, **1993**, pp. 465–496.
[82] A. Rich, *Gene* **1993**, *195*, 99–109.
[83] K. Yanagi, G. G. Privé, R. E. Dickerson, *J. Mol. Biol.* **1991**, *217*, 201–214.
[84] W. Saenger, W. N. Hunter, O. Kennard, *Nature* **1986**, *324*, 385–388.
[85] H. M. Berman, *Curr. Opin. Struct. Biol.* **1991**, *1*, 423–427.
[86] J. Doucet, J.-P. Benoit, W. B. T. Cruse, T. Prange, O. Kennard, *Nature* **1989**, *337*, 190–192.
[87] Z. Shakked, G. Guerstein-Guzikevich, M. Eisenstein, F. Frolow, D. Rabinovich, *Nature* **1989**, *342*, 456–460.
[88] S. Jain, M. J. Sundaralingam, *J. Biol. Chem.* **1989**, *264*, 12780–12784.
[89] A. Lipanov, M. L. Kopka, M. Kaczor-Grzeskowiak, J. Quintana, R. E. Dickerson, *Biochemistry* **1993**, *32*, 1373–1389.
[90] L. Nekludova, C. O. Pabo, *Proc. Natl. Acad. Sci. USA* **1994**, *91*, 6948–6952.
[91] O. Kennard, W. N. Hunter, *Angew. Chem.* **1991**, *103*, 1280–1304, *Angew. Chem. Int. Ed. Engl.* **1991**, *30*, 1254–1277.
[92] R. E. Dickerson in *Methods in Enzymology, Vol. 211* (Eds.: D. M. J. Lilley, J. E. Dahlberg), Academic Press, San Diego, **1992**, pp. 67–111.
[93] L. Joshua-Tor, J. L. Sussman, *Curr. Opin. Struct. Biol.* **1993**, *3*, 323–335.
[94] M. Egli in *Structure Correlation* (Eds.: H.-B. Bürgi, J. D. Dunitz), VCH, New York, **1994**, pp. 705–749.

[95] A. Rich in *The Chemical Bond: Structure and Dynamics* (Ed.: A. Zewail), Academic Press, New York, **1992**, pp. 31–85.
[96] P. B. Sigler, *Proc. Robert A. Welch Found.* **1993**, *37*, pp. 63–76.
[97] T. A. Steitz, *Structural Studies of Protein-Nucleic Acid Interaction*, Cambridge University Press, Cambridge, **1993**.
[98] *Curr. Opin. Struct. Biol.* **1994**, *4*, 1–66.
[99] W. Saenger, *Principles of Nucleic Acid Structure*, 1st ed., Springer, New York, **1986**.
[100] H. M. Berman, W. K. Olson, D. L. Beveridge, J. Westbrook, A. Gelbin, T. Demeny, S.-H. Hsieh, A. R. Srinivasan, B. Schneider, *Biophys. J.* **1992**, *63*, 751–759.
[101] K. B. Hall, L. W. McLaughlin, *Biochemistry* **1991**, *30*, 10606–10613.
[102] M. Egli, S. Portmann, D. Tracz, C. Workman, N. Usman, *Acta Crystallogr. Sect. D* **1995**, *51*, 1065–1070
[103] S. Portmann, N. Usman, M. Egli, *Biochemistry* **1995**, *34*, 7569–7575; M. Egli, S. Portmann, N. Usman, *ibid.* **1996**, *35*, 8489–8494.
[104] M. Egli, N. Usman, S. Zhang, A. Rich, *Proc. Natl. Acad. Sci. USA* **1992**, *89*, 534–538.
[105] M. Egli, N. Usman, A. Rich, *Biochemistry* **1993**, *32*, 3221–3237.
[106] P. Lubini, W. Zürcher, M. Egli, *Chem. Biol.* **1994**, *1*, 39–45.
[107] R. Wing, H. Drew, T. Takano, C. Broka, S. Tanaka, K. Itakura, R. E. Dickerson, *Nature* **1980**, *287*, 755–758.
[108] A.-H. Wang, Y.-G. Gao in *Methods, Vol. 1* (Eds.: J. N. Abelson, M. I. Simon), Academic Press, San Diego, **1990**, pp. 91–99.
[109] A. C. Dock-Bregeon, D. Moras in *Crystallization of Nucleic Acids and Proteins* (Eds.: A. Ducruix, R. Giegé), Oxford University Press, Oxford, **1992**, pp. 145–174.
[110] J. Jancarik, S.-H. Kim, *J. Appl. Crystallogr.* **1991**, *24*, 409–411.
[111] *Hampton Research Crystallization News* **1995**, *5*, No. 1.
[112] J. A. Doudna, C Grosshans, A. Gooding, C. E. Kundrot, *Proc. Natl. Acad. Sci. USA* **1993**, *90*, 7829–7833.
[113] W. G. Scott, J. T. Finch, R. Grenfell, J. Fogg, T. Smith, M. J. Gait, A. Klug, *J. Mol. Biol.* **1995**, 250, 327–332.
[114] K. J. Baeyens, J. Jancarik, S. R. Holbrook, *Acta Crystallogr. Sect. D* **1994**, *50*, 764–767.
[115] R. V. Gessner, G. J. Quigley, M. Egli, *J. Mol. Biol.* **1994**, *236*, 1154–1168.
[116] H. R. Drew, R. E. Dickerson, *J. Mol. Biol.* **1981**, *151*, 535–556.
[117] M. L. Kopka, A. V. Fratini, H. R. Drew, R. E. Dickerson, *J. Mol. Biol.* **1983**, *163*, 129–146.
[118] K. C. Schneider, S. A. Benner, *J. Am. Chem. Soc.* **1990**, *112*, 453–455.
[119] J. Hunziker, H.-R. Roth, M. Böhringer, A. Giger, U. Diedrichsen, M. Göbel, R. Krishnan, B. Jaun, C. Leumann, A. Eschenmoser, *Helv. Chim. Acta* **1993**, *76*, 259–352.
[120] R. J. Jones, S. Swaminathan, J. F. Milligan, S. Wadwani, B. C. Froehler, M. D. Matteucci, *J. Am. Chem. Soc.* **1993**, *115*, 9816–9817.
[121] K.-H. Altmann, R. Kesselring, E. Francotte, G. Rihs, *Tetrahedron Lett.* **1994**, *35*, 2331–2334.
[122] K.-H. Altmann, R. Imwinkelried, R. Kesselring, G. Rihs, *Tetrahedron Lett.* **1994**, *35*, 7625–7628.
[123] M. Tarköy, M. Bolli, C. Leumann, *Helv. Chim. Acta* **1994**, *77*, 716–744.
[124] M. Egli, P. Lubini, M. Bolli, M. Dobler, C. Leumann, *J. Am. Chem. Soc.* **1993**, *115*, 5855–5856.
[125] P. Lubini, M. Egli in *Structural Biology: The State of the Art, Proceedings of the Eighth Conversation, Vol. 2* (Eds.: R. H. Sarma, M. H. Sarma), Adenine Press, Schenectady, NY, **1994**, pp. 155–175.
[126] K. Gehring, J.-L. Leroy, M. Guéron, *Nature* **1993**, *363*, 561–565; L. Chen, L. Cai, X. Zhang, A. Rich, *Biochemistry* **1994**, *33*, 13540–13546; C. H. Kang, I. Berger, C. Lockshin, R. Ratliff, R. Moyzis, A. Rich, *Proc. Natl. Acad. Sci. USA* **1994**, *91*, 11636–11640; J.-L. Leroy, M. Guéron, *Structure* **1995**, *3*, 101–120; I. Berger, C. H. Kang, A. Fredian, R. Ratliff, R. Moyzis, A. Rich, *Nature Struct. Biol.* **1995**, *2*, 416–425; C. H. Kang, I. Berger, C. Lockshin, R. Ratliff, R. Moyzis, A. Rich, *Proc. Natl. Acad. Sci. USA* **1995**, *92*, 3874–3878.
[127] I. Berger, M. Egli, A. Rich, *Proc. Natl. Acad. Sci. USA* **1996**, *93*, in press.
[128] D. M. Crothers, *Science* **1994**, *266*, 1819–1820, and references therein.
[129] Z. Huang, K. C. Schneider, S. A. Benner in *Antisense Nucleotide Analogs* (Ed.: S. Agrawal), Humana Press, Totawa, NJ, **1993**, pp. 315–353.
[130] C. Richert, A. L. Roughton, S. A. Benner, *J. Am. Chem. Soc.* **1996**, *118*, 4518–4531.
[131] A. L. Roughton, S. Portmann, S. A. Benner, M. Egli, *J. Am. Chem. Soc.* **1995**, *117*, 7249–7250.
[132] R. O. Day, N. C. Seeman, J. M. Rosenberg, A. Rich, *Proc. Natl. Acad. Sci. USA* **1973**, *70*, 849–853.
[133] J. M. Rosenberg, N. C. Seeman, R. O. Day, A. Rich, *J. Mol. Biol.* **1976**, *104*, 145–167.
[134] N. P. Johnson, T. Schleich, *Biochemistry* **1974**, *13*, 981–987.
[135] R. R. Breaker, G. R. Gough, P. T. Gilham, *Biochemistry* **1993**, *32*, 9125–9128.
[136] S. P. Collingwood, A. D. Baxter, *Synlett* **1995**, 703–705.
[137] B. Hyrup, C. Richert, T. Schulte-Herbrüggen, S. A. Benner, M. Egli, *Nucleic Acids Res.* **1995**, *23*, 2427–2433.
[138] Review: S. L. Beaucage, R. P. Iyer, *Tetrahedron* **1993**, *49*, 6123–6194.
[139] S. Portmann, K.-H. Altmann, N. Reynes, M. Egli, *J. Am. Chem. Soc.*, submitted.
[140] R. E. Dickerson, H. R. Drew, *J. Mol. Biol.* **1981**, *149*, 761–786.
[141] H. R. Drew, R. M. Wing, T. Takano, C. Broka, S. Tanaka, K. Itakura, R. E. Dickerson, *Proc. Natl. Acad. Sci. USA* **1981**, *78*, 2179–2183.
[142] K.-H. Altmann CIBA AG, personal communication.
[143] B. S. Sproat, A. I. Lamond, B. Beijer, P. Neuner, U. Ryder, *Nucleic Acids Res.* **1989**, *17*, 3373–3386.
[144] C. Schmit, M.-O. Bévierre, A. De Mesmaeker, K.-H. Altmann, *Bioorg. Med. Chem. Lett.* **1994**, *4*, 1969–1974.
[145] T. E. Haran, Z. Shakked, A. H.-J. Wang, A. Rich, *J. Biomol. Struct. Dyn.* **1987**, *5*, 199–217.
[146] M. Eisenstein, Z. Shakked, *J. Mol. Biol.* **1995**, *248*, 662–678.
[147] A. M. Kawasaki, M. D. Casper, S. M. Freier, E. A. Lesnik, M. C. Zounes, L. L. Cummins, C. Gonzalez, P. D. Cook, *J. Med. Chem.* **1993**, *36*, 831–841.
[148] C. Mattos, B. Rasmussen, X. Ding, G. A. Petsko, D. Ringe, *Nature Struct. Biol.* **1994**, *1*, 55–58.
[149] R. Taylor, J. D. Dunitz, unpublished results.
[150] S. Wang, E. T. Kool, *Biochemistry* **1995**, *34*, 4125–4132.
[151] J. Hall, D. Hüsken, U. Pieles, H. E. Moser, R. Häner, *Chem. Biol.* **1994**, *1*, 185–190, and references therein.
[152] N. Usman, R. Cedergren, *Trends Biochem. Sci.* **1992**, *17*, 334–339, and references therein.
[153] N. Usman, D. T. Stinchcomb, *Nucleic Acids Mol. Biol.* **1995**, *10*, 243–264, and references therein.
[154] F. H. Westheimer, *Acc. Chem. Res.* **1968**, *1*, 70–78.
[155] D. A. Usher, A. H. McHale, *Proc. Natl. Acad. Sci. USA* **1976**, *73*, 1149–1153.
[156] R. S. Brown, J. C. Dervan, A. Klug, *Biochemistry* **1985**, *24*, 4785–4801.
[157] D. Hüsken, G. Goodall, R. Häner, H. E. Moser, unpublished results.
[158] H. W. Pley, K. M. Flaherty, D. B. McKay, *Nature* **1994**, *372*, 68–74.
[159] A. H.-J. Wang, S. Fujii, J. H. van Boom, G. A. van der Marel, S. A. A. van Boeckel, A. Rich, *Nature* **1982**, *299*, 601–604.
[160] S. Portmann, S. Grimm, C. Workman, N. Usman, M. Egli, *Chem. Biol.* **1996**, *3*, 173–184.
[161] H.-N. Wu, O. C. Uhlenbeck, *Biochemistry* **1987**, *26*, 8221–8227.
[162] F. Michel, M. Hanna, R. Green, D. P. Bartel, J. W. Szostak, *Nature* **1989**, *342*, 391–395.
[163] A. Jacquier, *Trends Biochem. Sci.* **1990**, *15*, 351–354.
[164] K. Valegård, J. B. Murray, P. G. Stockley, N. J. Stonehouse, L. Liljas, *Nature* **1994**, *371*, 623–626.
[165] C. C. Query, M. J. Moore, P. A. Sharp, *Genes Dev.* **1994**, *8*, 587–597.
[166] K. H. Altmann, N. M. Dean, D. Fabbro, S. M. Freier, T. Geiger, R. Häner, D. Hüsken, P. Martin, B. P. Monia, M. Müller, F. Natt, P. Nicklin, J. Phillips, U. Pieles, H. Sasmor, H. E. Moser, *Chimia* **1996**, *50*, 168–176.
[167] C. Moulds, J. G. Lewis, B. C. Fröhler, D. Grant, T. Huang, J. F. Milligan, M. D. Matteucci, R. W. Wagner, *Biochemistry* **1995**, *34*, 5044–5053.